Diffractive electroproduction of vector mesons on nuclei at EIC

Jan Nemchik
Czech Technical University in Prague, FNSPE, Prague, Czech Republic
Institute of Experimental Physics SAS, Košice, Slovakia

Physics Opportunities at an Electron-Ion Collider, POETIC 2013

4-8 March 2013, Universidad Técnica Federíco Santa María, Valparaíso, CHILE

In collaboration with

B. Kopeliovich, N. Nikolaev, A. Tarasov, B. Zakharov

Outline

- **Nuclear effects**

Outline

- **Nuclear effects**
  - $\Rightarrow$ color transparency (CT)

Outline

- **Nuclear effects**
  - ⇒ color transparency (CT)
  - ⇒ quantum coherence - coherence length (CL)

Outline

- **Nuclear effects**
  - $\Rightarrow$ color transparency (CT)
  - $\Rightarrow$ quantum coherence - coherence length (CL)
  - $\Rightarrow$ different regimes of VM production

Outline

- **Nuclear effects**
  - ⇒ color transparency (CT)
  - ⇒ quantum coherence - coherence length (CL)
  - ⇒ different regimes of VM production
  - ⇒ CT-CL mixing

Outline

- **Nuclear effects**
  - $\Rightarrow$ color transparency (CT)
  - $\Rightarrow$ quantum coherence - coherence length (CL)
  - $\Rightarrow$ different regimes of VM production
  - $\Rightarrow$ CT-CL mixing
- **Color dipole phenomenology** $\Rightarrow$ Green f. formalism

Outline

- **Nuclear effects**
  - $\Rightarrow$ color transparency (CT)
  - $\Rightarrow$ quantum coherence - coherence length (CL)
  - $\Rightarrow$ different regimes of VM production
  - $\Rightarrow$ CT-CL mixing
- **Color dipole phenomenology** $\Rightarrow$ Green f. formalism
- **Gluon shadowing**

Outline

- Nuclear effects
  - ⇒ color transparency (CT)
  - ⇒ quantum coherence - coherence length (CL)
  - ⇒ different regimes of VM production
  - ⇒ CT-CL mixing
- Color dipole phenomenology ⇒ Green f. formalism
- Gluon shadowing
- Numerical results vs data

  ⇒ comparison with CLAS data at JLab
  ⇒ comparison with HERMES data
  ⇒ comparison with E665 data
  ⇒ perspectives for EIC

Outline

- **Nuclear effects**
  - ⇒ color transparency (CT)
  - ⇒ quantum coherence - coherence length (CL)
  - ⇒ different regimes of VM production
  - ⇒ CT-CL mixing
- **Color dipole phenomenology** ⇒ Green f. formalism
- **Gluon shadowing**
- **Numerical results vs data**

  ⇒ comparison with CLAS data at JLab

  ⇒ comparison with HERMES data

  ⇒ comparison with E665 data

  ⇒ perspectives for EIC
- **Summary & Outlook**

Nuclear effects

Color transparency

- COLOR TRANSPARENCY (CT) - one of the fundamental phenomena coming from the QCD

Nuclear effects

Color transparency

- COLOR TRANSPARENCY (CT) - one of the fundamental phenomena coming from the QCD
- CT was predicted to occur already in 1981

  [A.B. Zamolodchikov, B.Z. Kopeliovich and L.I. Lapidus, *Pis'ma Zh. Eksp. Teor. Fiz.* **33**, 612 (1981); *Sov. Phys. JETP Lett.* **33**, 595 (1981).]

  [G. Bertsch, S.J. Brodsky, A.S. Goldhaber and J.F. Gunion, *Phys. Rev. Lett.* **47**, 297 (1981).]

  in diffractive interaction with nuclei.

Nuclear effects

Color transparency

- COLOR TRANSPARENCY (CT) - one of the fundamental phenomena coming from the QCD
- CT was predicted to occur already in 1981

  [A.B. Zamolodchikov, B.Z. Kopeliovich and L.I. Lapidus, *Pis'ma Zh. Eksp. Teor. Fiz.* **33**, 612 (1981); *Sov. Phys. JETP Lett.* **33**, 595 (1981).]

  [G. Bertsch, S.J. Brodsky, A.S. Goldhaber and J.F. Gunion, *Phys. Rev. Lett.* **47**, 297 (1981).]

  in diffractive interaction with nuclei.
- The CT phenomenon is manifested as a vanishing interaction cross section $\sigma_{\bar{q}q}(r) \propto r^2$ for vanishing hadron (quark configuration) transverse size r.

Nuclear effects

Color transparency

- COLOR TRANSPARENCY (CT) - one of the fundamental phenomena coming from the QCD
- CT was predicted to occur already in 1981

  [A.B. Zamolodchikov, B.Z. Kopeliovich and L.I. Lapidus, *Pis'ma Zh. Eksp. Teor. Fiz.* **33**, 612 (1981); *Sov. Phys. JETP Lett.* **33**, 595 (1981).]

  [G. Bertsch, S.J. Brodsky, A.S. Goldhaber and J.F. Gunion, *Phys. Rev. Lett.* **47**, 297 (1981).]

  in diffractive interaction with nuclei.
- The CT phenomenon is manifested as a vanishing interaction cross section $\sigma_{\bar{q}q}(r) \propto r^2$ for vanishing hadron (quark configuration) transverse size r.
- The nuclear medium is more transparent for smaller transverse size of the hadron (quark configurations).

Nuclear effects

Color transparency

- Only a few experiments were able to confirm the CT :
  – PROZA experiment at Serpukhov, in quasi-free charge-exchange pion scattering of nuclei, at an energy of 40 GeV.
  – E791 experiment in diffractive coherent dissociation of pions on nuclei.

Nuclear effects

Color transparency

- Only a few experiments were able to confirm the CT :
  – PROZA experiment at Serpukhov, in quasi-free charge-exchange pion scattering of nuclei, at an energy of 40 GeV.
  – E791 experiment in diffractive coherent dissociation of pions on nuclei.
- An observation of the onset of CT in virtual diffractive photoproduction of ρ mesons was claimed by the E665 collaboration in 1995, measuring the Q^2-dependence of nuclear transparency defined as:

$$Tr_A^{inc(coh)} = \frac{\sigma^{inc(coh)}_{\gamma^* A \to V X(A)}}{A\, \sigma_{\gamma^* N \to V X}}$$

for the diffractive incoherent [quasielasic] $\gamma^* A \to V X$ and coherent [elastic] $\gamma^* A \to V A$ production of VMs.

Nuclear effects

Color transparency

The observed signal of CT by the E665 collaboration had been predicted as a rising nuclear transparency (vanishing final state interaction) with increasing hardness of the reaction Q^2.

[B.Z. Kopeliovich, J. Nemchik, N.N. Nikolaev,B.G. Zakharov, *Phys. Lett.* **B309**, 179 (1993).]

[B.Z. Kopeliovich, J. Nemchik, N.N. Nikolaev,B.G. Zakharov, *Phys. Lett.* **B324**, 469 (1994).]

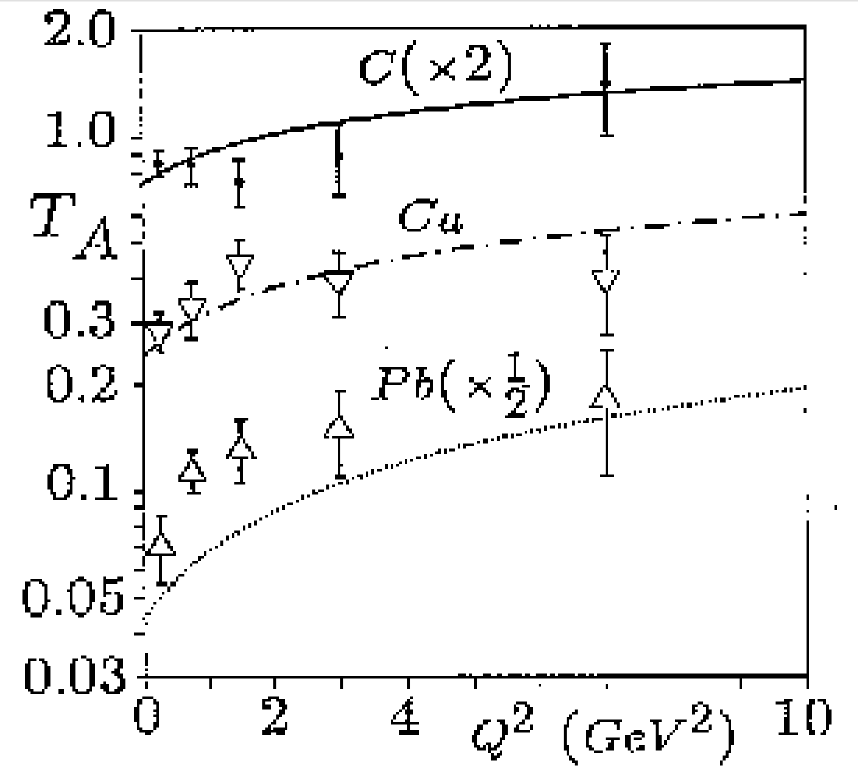

Nuclear effects

Color transparency

- Description of CT in electroproduction of vector mesons is realized within the quark-gluon representation

Nuclear effects

Color transparency

- Description of CT in electroproduction of vector mesons is realized within the quark-gluon representation
- Here a photon of high virtuality Q^2 is expected to produce a $\bar{q}q$ pair with a mean transverse separation

$$\langle r \rangle \sim \frac{1}{\sqrt{Q^2\alpha(1-\alpha)+m_q^2}}$$

asymmetric pairs are suppressed by the distribution function of L photons $\Rightarrow$ smaller transverse size than fluctuations of T photons, $\langle r \rangle_L < \langle r \rangle_T$.

Nuclear effects

Color transparency

- Description of CT in electroproduction of vector mesons is realized within the quark-gluon representation
- Here a photon of high virtuality Q^2 is expected to produce a $\bar{q}q$ pair with a mean transverse separation

$$\langle r \rangle \sim \frac{1}{\sqrt{Q^2 \alpha(1-\alpha) + m_q^2}}$$

asymmetric pairs are suppressed by the distribution function of L photons $\Rightarrow$ smaller transverse size than fluctuations of T photons, $\langle r \rangle_L < \langle r \rangle_T$.

- Then CT manifests itself as a vanishing absorption of the small size colorless $\bar{q}q$ wave packet during propagation through the nucleus.

Nuclear effects

Color transparency

- The dynamical evolution of the small size $\bar{q}q$ pair to a normal size vector meson is controlled by the time scale - formation time. Due to uncertainty principle, one needs a time interval to resolve different levels V (the ground state) or V' (the next excited state) in the final state. In the rest frame of the nucleus this formation time is Lorentz dilated,

$$t_f = \frac{2\,\nu}{m_{V'}{}^2 - m_V^2}\,.$$

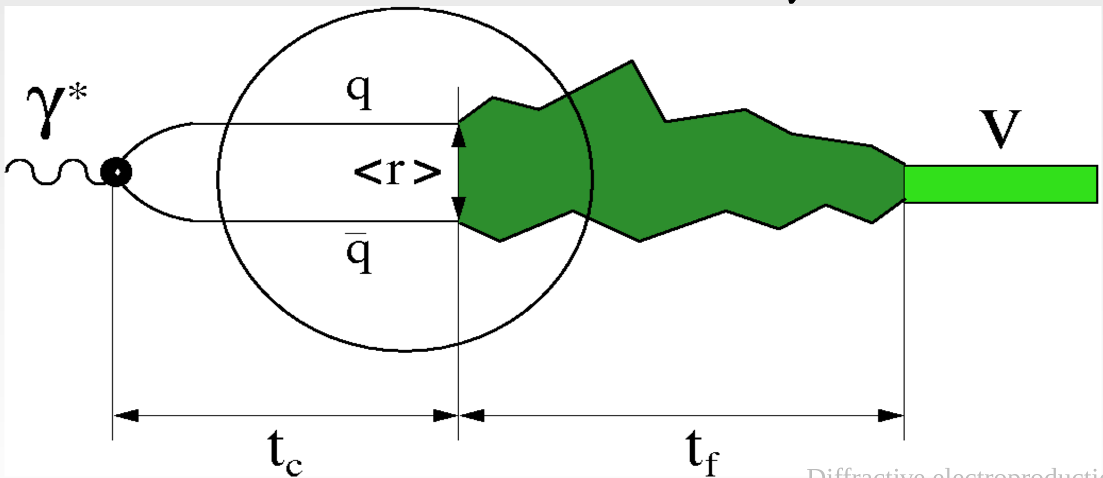

Nuclear effects

Quantum coherence

- Can be characterized by the lifetime of the $\bar{q}q$ fluctuations. It results from destructive interference of the amplitudes for which the interaction takes place on different bound nucleons. It is characterized by the coherence length (CL), which is related to the longitudinal momentum transfer by $q_c = 1/l_c$. It corresponds to the coherence time ($l_c = t_c$)

$$t_c = \frac{2\,\nu}{Q^2 + m_V^2}\,.$$

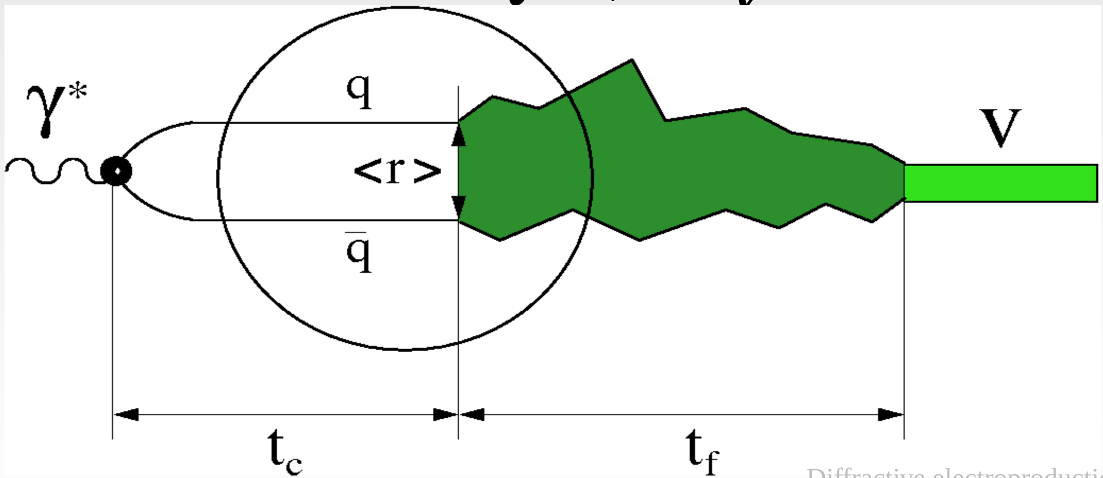

Nuclear effects

Different regimes of VM production

- 1. Small energy $t_c \sim t_f \to 0 \Rightarrow$ production of light vector mesons $\Rightarrow$ Nuclear transparency is given by the Glauber formula

  As energy rises, since $t_c \sim t_f \Rightarrow$ CT-CL mixing

Nuclear effects

Different regimes of VM production

- 1. Small energy $t_c \sim t_f \rightarrow 0 \Rightarrow$ production of light vector mesons $\Rightarrow$ Nuclear transparency is given by the Glauber formula
  As energy rises, since $t_c \sim t_f \Rightarrow$ CT-CL mixing
- 2. Small energy $t_c \sim 0$ BUT $t_f \sim R_A \Rightarrow$ production of heavy vector mesons $\Rightarrow$ nuclear suppression is caused by the evolution of the pair propagating through the nucleus.
  As energy rises, since $t_c < t_f \Rightarrow$ CT-CL mixing is important at larger energies in comparison with light VMs.
  [B.Z. Kopeliovich, B.G. Zakharov, *Phys. Rev.* **D44**, 3466 (1991).]

Nuclear effects

Different regimes of VM production

- 3. High energy limit $t_c, t_f \gg R_A \Rightarrow$ transverse $\bar{q}q$ separation are "frozen" by Lorentz time dilation during propagation through the nucleus $\Rightarrow$ nuclear suppression is given by the $\bar{q}q$ attenuation with a constant absorption cross section.

Nuclear effects

Different regimes of VM production

- 3. High energy limit $t_c, t_f \gg R_A \Rightarrow$ transverse $\bar{q}q$ separation are “frozen” by Lorentz time dilation during propagation through the nucleus $\Rightarrow$ nuclear suppression is given by the $\bar{q}q$ attenuation with a constant absorption cross section.
- 4. General case with no resrictions for either t_c or t_f. $\Rightarrow$ CT-CL mixing plays an important role.

Nuclear effects

CT-CL mixing

Elimination of CL effects

- 1. Investigation of $Tr_A(Q^2)$ as function of Q^2 at large energy, when $l_c, l_f \gg R_A$.
  E665 experiment, EIC

Nuclear effects

CT-CL mixing

Elimination of CL effects

- 1. Investigation of $Tr_A(Q^2)$ as function of Q^2 at large energy, when $l_c, l_f \gg R_A$.
  E665 experiment, EIC
- 2. Simple prescription for the elimination of CL effects from the data on the $Tr_A(Q^2)$ $\Rightarrow$ one should bin the data keeping $l_c = const$ $\Rightarrow$ ν and Q^2 should be correlated,

$$\nu = \frac{1}{2}\, l_c\,(Q^2 + m_V^2)\,.$$

In this case any rise with Q^2 of the nuclear transparency ratio is a clear signal of CT.

[J. Hüfner and B.Z. Kopeliovich, *Phys. Lett.* **B403**, 128 (1997)]

HERMES experiment, EIC at large Q^2

Nuclear effects

CT-CL mixing

Elimination of CL effects

- 3. Investigation of $Tr_A(Q^2)$ as function of Q^2 at small energy, when $l_c \ll R_A$. For this reason CL effects are expected to be much weaker than CT and CL-CT mixing does not play an important role. Therefore the study of vector meson electroproduction at small energies represents an alternative way for investigating a clear signal of CT.
CLAS experiment at JLab

Nuclear effects

CT-CL mixing

Elimination of CL effects

$$\nu = \frac{1}{2}\, l_c \,(Q^2 + m_V^2)\,.$$

CT effects are found to be much stronger at low (HERMES, CLAS) than at high (E665, EIC) energies:

— At high energies the CL l_c is long $\Rightarrow$ the FL is long too, $l_f \gtrsim l_c \gg R_A \Rightarrow$ nuclear transparency rises with Q^2 only because the mean transverse size of the $\bar{q}q$ photon fluctuations decreases.

— At lower energies when $l_c \lesssim R_A \Rightarrow$ the photon energy rises with Q^2 and consequently the FL rises as well. Thus, these two effects add up leading to a steeper growth of $Tr_A^{inc}(Q^2)$ for short l_c.

Basic formulas from the CDP

In the light-cone (LC) dipole approach for the process $\gamma^* N \to V\ N$ a diffractive process is treated as elastic scattering of a $\bar{q}q$ fluctuation of the incident particle. The forward production amplitude can be represented in the quantum-mechanical form

$$\mathcal{M}_{\gamma^* N \to V N}(s, Q^2) \; = \; \langle\, V |\, \sigma_{\bar{q}q}(\vec{r}, s)\, |\gamma^*\, \rangle \; =$$

$$\int\limits_0^1 d\alpha \int d^2 r \;\; \Psi^*_V(\vec{r}, \alpha)\, \sigma_{\bar{q}q}(\vec{r}, s)\, \Psi_{\gamma^*}(\vec{r}, \alpha, Q^2)$$

with the normalization

$$\left.\frac{d\sigma(\gamma^* N \to V N)}{dt}\right|_{t=0} = \frac{|\mathcal{M}_{\gamma^* N \to V N}(s, Q^2)|^2}{16\,\pi}.$$

Basic formulas from the CDP

Ingredients contributing to the amplitude

[B.Z. Kopeliovich, J. Nemchik, A. Schaefer, A.V. Tarasov, *Phys. Rev.* **C65**, 035201 (2002).]

- The dipole cross section $\sigma_{\bar{q}q}(\vec{r}, s)$ which depends on the $\bar{q}q$ transverse separation $\vec{r}$ and the c.m. energy squared s.

We explicitly consider the nonperturbative interaction effects between the q and $\bar{q}$, which can be included in the LC wave function of the photon, $\Psi_{\gamma^*}(\vec{r}, \alpha, Q^2)$.

Basic formulas from the CDP

Ingredients contributing to the amplitude

[B.Z. Kopeliovich, J. Nemchik, A. Schaefer, A.V. Tarasov, *Phys. Rev.* **C65**, 035201 (2002).]

- The dipole cross section $\sigma_{\bar{q}q}(\vec{r}, s)$ which depends on the $\bar{q}q$ transverse separation $\vec{r}$ and the c.m. energy squared s.
- The LC wave function of the photon, $\Psi_{\gamma^*}(\vec{r}, \alpha, Q^2)$, which besides the $\vec{r}$ dependence, depends also on the photon virtuality Q^2 and the relative share α of the photon momentum carried by the quark.

We explicitly consider the nonperturbative interaction effects between the q and $\bar{q}$, which can be included in the LC wave function of the photon, $\Psi_{\gamma^*}(\vec{r}, \alpha, Q^2)$.

Basic formulas from the CDP

Ingredients contributing to the amplitude

[B.Z. Kopeliovich, J. Nemchik, A. Schaefer, A.V. Tarasov, *Phys. Rev.* **C65**, 035201 (2002).]

- The dipole cross section $\sigma_{\bar{q}q}(\vec{r}, s)$ which depends on the $\bar{q}q$ transverse separation $\vec{r}$ and the c.m. energy squared s.
- The LC wave function of the photon, $\Psi_{\gamma^*}(\vec{r}, \alpha, Q^2)$, which besides the $\vec{r}$ dependence, depends also on the photon virtuality Q^2 and the relative share α of the photon momentum carried by the quark.
- The LC wave function of the vector meson $\Psi_V(\vec{r}, \alpha)$.

We explicitly consider the nonperturbative interaction effects between the q and $\bar{q}$, which can be included in the LC wave function of the photon, $\Psi_{\gamma^*}(\vec{r}, \alpha, Q^2)$.

Basic formulas from the CDP

- The Green function $G_{\bar{q}q}(z_1, \vec{r}_1; z_2, \vec{r}_2)$ describes the propagation of an interacting $\bar{q}q$ pair between points with longitudinal coordinates z_1 and z_2 and with initial and final transverse separations $\vec{r}_1$ and $\vec{r}_2$, and satisfies the two-dimensional Schrödinger equation,

Basic formulas from the CDP

- The Green function $G_{\bar{q}q}(z_1, \vec{r}_1; z_2, \vec{r}_2)$ describes the propagation of an interacting $\bar{q}q$ pair between points with longitudinal coordinates z_1 and z_2 and with initial and final transverse separations $\vec{r}_1$ and $\vec{r}_2$, and satisfies the two-dimensional Schrödinger equation,
-

$$i\frac{d}{dz_2} G_{\bar{q}q}(z_1, \vec{r}_1; z_2, \vec{r}_2) =$$

$$\left\{ \frac{\epsilon^2 - \Delta_{r_2}}{2\,\nu\,\alpha\,(1-\alpha)} + V_{\bar{q}q}(z_2, \vec{r}_2, \alpha) \right\} G_{\bar{q}q}(z_1, \vec{r}_1; z_2, \vec{r}_2)$$

Basic formulas from the CDP

- The Green function $G_{\bar{q}q}(z_1, \vec{r}_1; z_2, \vec{r}_2)$ describes the propagation of an interacting $\bar{q}q$ pair between points with longitudinal coordinates z_1 and z_2 and with initial and final transverse separations $\vec{r}_1$ and $\vec{r}_2$, and satisfies the two-dimensional Schrödinger equation,
- $$i\frac{d}{dz_2} G_{\bar{q}q}(z_1, \vec{r}_1; z_2, \vec{r}_2) =$$
$$\left\{ \frac{\epsilon^2 - \Delta_{r_2}}{2\,\nu\,\alpha\,(1-\alpha)} + V_{\bar{q}q}(z_2, \vec{r}_2, \alpha) \right\} G_{\bar{q}q}(z_1, \vec{r}_1; z_2, \vec{r}_2)$$
- with the boundary condition
$$G_{\bar{q}q}(z_1, \vec{r}_1; z_2, \vec{r}_2)|_{z_2=z_1} = \delta^2(\vec{r}_1 - \vec{r}_2).$$

Basic formulas from the CDP

- The real part of the LC potential $V_{\bar{q}q}(z_2, \vec{r}_2, \alpha)$ is responsible for the interaction between the q and $\bar{q}$ in the vacuum. If one takes the oscillator form of the potential,

Basic formulas from the CDP

- The real part of the LC potential $V_{\bar{q}q}(z_2, \vec{r}_2, \alpha)$ is responsible for the interaction between the q and $\bar{q}$ in the vacuum. If one takes the oscillator form of the potential,
- $$\mathrm{Re}\, V_{\bar{q}q}(z_2, \vec{r}_2, \alpha) = \frac{a^4(\alpha)\, \vec{r}_2^{\;2}}{2\,\nu\,\alpha(1-\alpha)}\,,$$

Basic formulas from the CDP

- The real part of the LC potential $V_{\bar{q}q}(z_2, \vec{r}_2, \alpha)$ is responsible for the interaction between the q and $\bar{q}$ in the vacuum. If one takes the oscillator form of the potential,
- $$\mathrm{Re}\, V_{\bar{q}q}(z_2, \vec{r}_2, \alpha) = \frac{a^4(\alpha)\, \vec{r}_2^{\;2}}{2\,\nu\,\alpha(1-\alpha)}\,,$$
- this leads to a Gaussian r- dependence of the LC wave function of the meson ground state

$$\Psi_V(\vec{r}, \alpha) = C_V\, f(\alpha) \exp\left[-\frac{1}{2}\, a^2(\alpha)\, \vec{r}^{\;2}\right]\,.$$

[B.Z. Kopeliovich, A. Schäfer and A.V. Tarasov, *Phys. Rev.* **D62**, 054022 (2000).]

Basic formulas from the CDP

- The shape of the function $a(\alpha)$ reads,

$$a(\alpha) = 2a_1\sqrt{\alpha(1-\alpha)},$$

Basic formulas from the CDP

- The shape of the function $a(\alpha)$ reads,

$$a(\alpha) = 2a_1\sqrt{\alpha(1-\alpha)},$$

-

$$\begin{array}{llll} a_1 = 0.169\ \text{GeV} & for & \rho^0 & mesons \\ a_1 = 0.238\ \text{GeV} & for & \phi^0 & mesons \\ a_1 = 0.537\ \text{GeV} & for & J/\Psi & mesons \\ a_1 = 1.611\ \text{GeV} & for & \Upsilon & mesons \end{array}$$

[B.Z. Kopeliovich, A. Schäfer and A.V. Tarasov, *Phys. Rev.* **D62**, 054022 (2000).]

[J. Nemchik, N.N. Nikolaev, E. Predazzi and B.G. Zakharov, *Z. Phys.* **C75**, 71 (1997).]

Basic formulas from the CDP

- The oscillator form of $\mathrm{Re}\, V_{\bar{q}q}$ leads to an analytical solution of the Schroedinger equation with the following explicit form of the harmonic oscillator Green function

  [R.P. Feynman and A.R. Gibbs, *Quantum Mechanics and Path Integrals*, McGraw-Hill Book Company, NY 1965.]

$$G_{\bar{q}q}(z_1, \vec{r}_1; z_2, \vec{r}_2) = \frac{a^2(\alpha)}{2\,\pi\,i\,\sin(\omega\,\Delta z)} \times$$

$$\exp\left\{\frac{i\,a^2(\alpha)}{\sin(\omega\,\Delta z)}\left[(r_1^2 + r_2^2)\cos(\omega\;\Delta z) - 2\;\vec{r}_1\cdot\vec{r}_2\right]\right\}$$

$$\times \exp\left[-\frac{i\,\epsilon^2\,\Delta z}{2\,\nu\,\alpha\,(1-\alpha)}\right]\,,$$

Basic formulas from the CDP

- The oscillator form of $\mathrm{Re}\, V_{\bar{q}q}$ leads to an analytical solution of the Schroedinger equation with the following explicit form of the harmonic oscillator Green function

  [R.P. Feynman and A.R. Gibbs, *Quantum Mechanics and Path Integrals*, McGraw-Hill Book Company, NY 1965.]

$$G_{\bar{q}q}(z_1, \vec{r}_1; z_2, \vec{r}_2) = \frac{a^2(\alpha)}{2\,\pi\, i\, \sin(\omega\,\Delta z)} \times$$
$$\exp\left\{\frac{i\, a^2(\alpha)}{\sin(\omega\,\Delta z)}\left[(r_1^2 + r_2^2)\cos(\omega\;\Delta z) - 2\;\vec{r}_1\cdot\vec{r}_2\right]\right\}$$
$$\times\exp\left[-\frac{i\,\epsilon^2\,\Delta z}{2\,\nu\,\alpha\,(1-\alpha)}\right],$$

- $\Delta z = z_2 - z_1$ and $\omega = \frac{a^2(\alpha)}{\nu\,\alpha(1-\alpha)}$.

Basic formulas from the CDP

- Assuming s-channel helicity conservation, the forward production amplitude for the process $\gamma^* N \to V N$, separately for transverse (T) and longitudinal (L) photons and vector mesons, reads,

$$\mathcal{M}^T_{\gamma^* N \to V N}(s, Q^2)\Big|_{t=0} = N_C\, Z_q\, \sqrt{2\,\alpha_{em}} \int d^2 r\, \sigma_{\bar{q}q}(\vec{r}, s) \times$$

$$\int_0^1 d\alpha \Big\{ m_q^2 \Phi_0(\epsilon, \vec{r}, \lambda) \Psi_V^T(\vec{r}, \alpha) - [\alpha^2 + (1-\alpha)^2] \vec{\Phi}_1(\epsilon, \vec{r}, \lambda) \cdot \vec{\nabla}_r \Psi_V^T(\vec{r}, \alpha) \Big\} ;$$

$$\mathcal{M}^L_{\gamma^* N \to V N}(s, Q^2)\Big|_{t=0} = 4\, N_C\, Z_q\, \sqrt{2\,\alpha_{em}}\, m_V\, Q \;\times$$

$$\int d^2 r\, \sigma_{\bar{q}q}(\vec{r}, s) \int_0^1 d\alpha\, \alpha^2\, (1-\alpha)^2\, \Phi_0(\epsilon, \vec{r}, \lambda) \Psi_V^L(\vec{r}, \alpha) \,.$$

Basic formulas from the CDP

- The functions $\Phi_{0,1}$ include nonperturbative interaction effects between q and $\bar{q}$, and Ψ_V represents the vector meson wave function, whose explicit form is taken from [B.Z. Kopeliovich, J. Nemchik, A. Schaefer, A.V. Tarasov, *Phys. Rev.* **C65**, 035201 (2002).]

Basic formulas from the CDP

- The functions $\Phi_{0,1}$ include nonperturbative interaction effects between q and $\bar{q}$, and Ψ_V represents the vector meson wave function, whose explicit form is taken from [B.Z. Kopeliovich, J. Nemchik, A. Schaefer, A.V. Tarasov, *Phys. Rev.* **C65**, 035201 (2002).]

- Usually the data are presented in the form of the production cross section $\sigma = \sigma^T + \epsilon' \sigma^L$, at a given photon polarization ϵ'. Here the transverse and longitudinal cross sections, integrated over t, read:

$$\sigma^{T,L}(\gamma^* N \to V N) = \frac{|\mathcal{M}^{T,L}|^2}{16\pi\, B_{\gamma^* N}}\,,$$

where $B_{\gamma^* N}$ is the t-slope parameter in the differential cross section for reaction $\gamma^* N \to V N$.

Basic formulas from the CDP

- Since the t-slope of the differential quasielastic cross section is the same as on a nucleon target, instead of the integrated cross sections one can also use the forward differential cross sections to write

$$Tr_A^{inc} = \frac{1}{A}\left|\frac{\mathcal{M}_{\gamma^* A \to V X}(s,Q^2)}{\mathcal{M}_{\gamma^* N \to V N}(s,Q^2)}\right|^2 .$$

Basic formulas from the CDP

- Since the t-slope of the differential quasielastic cross section is the same as on a nucleon target, instead of the integrated cross sections one can also use the forward differential cross sections to write

$$Tr_A^{inc} = \frac{1}{A} \left| \frac{\mathcal{M}_{\gamma^* A \to V X}(s, Q^2)}{\mathcal{M}_{\gamma^* N \to V N}(s, Q^2)} \right|^2 .$$

- For coherent (elastic) production of vector mesons the t-slopes of the differential cross sections for nucleon and nuclear targets are different and do not cancel in the ratio. Therefore, the nuclear transparency also includes the slope parameter $B_{\gamma^* N}$ for the process $\gamma^* N \to V N$,

$$Tr_A^{coh} = \frac{\sigma_A^{coh}}{A\,\sigma_N} = \frac{16\,\pi\,B_{\gamma^* N}\,\sigma_A^{coh}}{A\,|\mathcal{M}_{\gamma^* N \to V N}(s, Q^2)\,|^2}$$

Basic formulas from the CDP

- Propagation of an interacting $\bar{q}q$ pair in a nuclear medium is also described by the Green function satisfying the evolution Schroedinger eq. However, the potential in this case acquires also an imaginary part which represents absorption in the medium,

$$Im V_{\bar{q}q}(z_2, \vec{r}, \alpha) = -\frac{\sigma_{\bar{q}q}(\vec{r}, s)}{2}\, \rho_A(b, z_2)\,,$$

Basic formulas from the CDP

- Propagation of an interacting $\bar{q}q$ pair in a nuclear medium is also described by the Green function satisfying the evolution Schroedinger eq. However, the potential in this case acquires also an imaginary part which represents absorption in the medium,

$$Im V_{\bar{q}q}(z_2, \vec{r}, \alpha) = -\frac{\sigma_{\bar{q}q}(\vec{r}, s)}{2}\, \rho_A(b, z_2)\,,$$

- $\rho_A(b, z)$ is the nuclear density function defined at given impact parameter b and longitudinal coordinate z.

Basic formulas from the CDP

- The analytical solution of the Schroedinger eq. is only known for the harmonic oscillator potential $V(r) \propto r^2$ using the dipole cross section approximation,

$$\sigma_{\bar{q}q}(r,s) = C(s)\, r^2 \, .$$

Basic formulas from the CDP

- The analytical solution of the Schroedinger eq. is only known for the harmonic oscillator potential $V(r) \propto r^2$ using the dipole cross section approximation,

$$\sigma_{\bar{q}q}(r,s) = C(s)\, r^2 \, .$$

- Then the solution of the Schroedinger eq. leads to the same explicit form of GF as in the vacuum, except that one should replace $\omega \Rightarrow \Omega$, where

$$\Omega = \frac{\sqrt{a^4(\alpha) - i\, \rho_A(b,z)\, \nu\, \alpha\, (1-\alpha)\, C(s)}}{\nu\, \alpha(1-\alpha)} \, .$$

Basic formulas from the CDP

Different regimes of VM production **(inc)**

- CL is much shorter than the mean nucleon spacing in a nucleus ($l_c \to 0$) $\Rightarrow G(z_2, \vec{r}_2; z_1, \vec{r}_1) \to \delta(z_2 - z_1)$. Correspondingly, the formation time t_f is very short. For light vector mesons $l_f \sim l_c$, and both must be short. Consequently, nuclear transparency is given by the simple formula corresponding to the Glauber approximation:

$$Tr_A^{inc} = \frac{1}{A} \int d^2b \int_{-\infty}^{\infty} dz\, \rho_A(b,z)\, \exp\left[-\sigma_{in}^{VN} \int_z^{\infty} dz'\, \rho_A(b,z')\right]$$

$$= \frac{1}{A\,\sigma_{in}^{VN}} \int d^2b \left\{1 - \exp\left[-\sigma_{in}^{VN}\, T_A(b)\right]\right\} = \frac{\sigma_{in}^{VA}}{A\,\sigma_{in}^{VN}}\,,$$

where σ_{in}^{VN} is the inelastic VN cross section.

Basic formulas from the CDP

Different regimes of VM production **(inc)**

- The production of charmonia and other heavy flavors $\Rightarrow$ intermediate case where as before $l_c \to 0$, but $l_f \sim R_A$. Then the formation of the meson wave function is described by the Green function, and the nuclear amplitude squared has the form

  [B.Z. Kopeliovich, B.G. Zakharov, *Phys. Rev.* **D44**, 3466 (1991).]

$$\left|\mathcal{M}_{\gamma^* A \to V X}(s,Q^2)\right|^2_{l_c \to 0;\, l_f \sim R_A} = \int d^2 b \int_{-\infty}^{\infty} dz\, \rho_A(b,z)\, \left|F_1(b,z)\right|^2 ,$$

$$F_1(b,z) = \int_0^1 d\alpha \int d^2 r_1\, d^2 r_2\, \Psi^*_V(\vec{r}_2,\alpha)\ \times$$

$$G(z',\vec{r}_2; z,\vec{r}_1)\, \sigma_{\bar{q}q}(r_1,s)\, \Psi_{\gamma^*}(\vec{r}_1,\alpha)\Big|_{z' \to \infty}$$

Basic formulas from the CDP

Different regimes of VM production **(inc)**

- In the high energy limit $l_c \gg R_A \Rightarrow$ $G(z_2,\vec{r}_2;z_1,\vec{r}_1) \to \delta(\vec{r}_2-\vec{r}_1) \Rightarrow$ all fluctuations of the transverse $\bar{q}q$ separation are "frozen" by Lorentz time dilation and the nuclear amplitude squared has the form

$$\left|\mathcal{M}_{\gamma^* A\to VX}(s,Q^2)\right|^2_{l_c\gg R_A} = \int d^2b\, T_A(b)\times$$

$$\left|\int d^2r\int_0^1 d\alpha\,\Psi_V^*(\vec{r},\alpha)\sigma_{\bar{q}q}(r,s)\exp\left[-\frac{1}{2}\sigma_{\bar{q}q}(r,s)T_A(b)\right]\Psi_{\gamma^*}(\vec{r},\alpha,Q^2)\right|^2$$

Basic formulas from the CDP

Different regimes of VM production **(inc)**

- In the high energy limit $l_c \gg R_A \Rightarrow$ $G(z_2, \vec{r}_2; z_1, \vec{r}_1) \to \delta(\vec{r}_2 - \vec{r}_1) \Rightarrow$ all fluctuations of the transverse $\bar{q}q$ separation are "frozen" by Lorentz time dilation and the nuclear amplitude squared has the form

$$\left|\mathcal{M}_{\gamma^* A \to V X}(s, Q^2)\right|^2_{l_c \gg R_A} = \int d^2 b\, T_A(b) \times$$

$$\left|\int d^2 r \int_0^1 d\alpha \Psi_V^*(\vec{r}, \alpha) \sigma_{\bar{q}q}(r, s) \exp\left[-\frac{1}{2} \sigma_{\bar{q}q}(r, s) T_A(b)\right] \Psi_{\gamma^*}(\vec{r}, \alpha, Q^2)\right|^2$$

- $\bar{q}q$ attenuates with a constant absorption cross section as in the Glauber model, except that the whole exponential is averaged rather than just the cross section in the exponent. The difference between the results of the two prescriptions are the well known inelastic corrections of Gribov

Basic formulas from the CDP

Different regimes of VM production $\mathbf{(inc)}$

- The general case when there are no restrictions for either l_c or l_f. Then the incoherent nuclear production amplitude squared is represented as a sum of two terms:

$$\Big|\mathcal{M}_{\gamma^* A\to VX}(s,Q^2)\Big|^2 = \int d^2b \int\limits_{-\infty}^{\infty} dz\, \rho_A(b,z)\,\Big|F_1(b,z) - F_2(b,z)\Big|^2 .$$

Basic formulas from the CDP

Different regimes of VM production **(inc)**

- The general case when there are no restrictions for either l_c or l_f. Then the incoherent nuclear production amplitude squared is represented as a sum of two terms:

$$\left|\mathcal{M}_{\gamma^* A \to V X}(s, Q^2)\right|^2 = \int d^2b \int_{-\infty}^{\infty} dz\, \rho_A(b, z) \left|F_1(b, z) - F_2(b, z)\right|^2 .$$

- The first term $F_1(b, z)$, introduced above corresponds to the short l_c limit. The second term $F_2(b, z)$ corresponds to the situation when the incident photon produces a $\bar{q}q$ pair diffractively and coherently at the point z_1, prior to an incoherent quasielastic scattering at point z. The LC Green function describes the evolution of the $\bar{q}q$ over the distance from z_1 to z and further on, up to the formation of the meson wave function.

Basic formulas from the CDP

Different regimes of VM production **(inc)**

$$F_2(b,z) = \frac{1}{2}\int_{-\infty}^{z} dz_1\,\rho_A(b,z_1)\int_0^1 d\alpha \int d^2r_1\,d^2r_2\,d^2r \;\times$$

$$\Psi^*_V(\vec{r}_2,\alpha)G(z',\vec{r}_2;z,\vec{r})\sigma_{\bar{q}q}(\vec{r},s)G(z,\vec{r};z_1,\vec{r}_1)\sigma_{\bar{q}q}(\vec{r}_1,s)\Psi_{\gamma^*}(\vec{r}_1,\alpha)$$

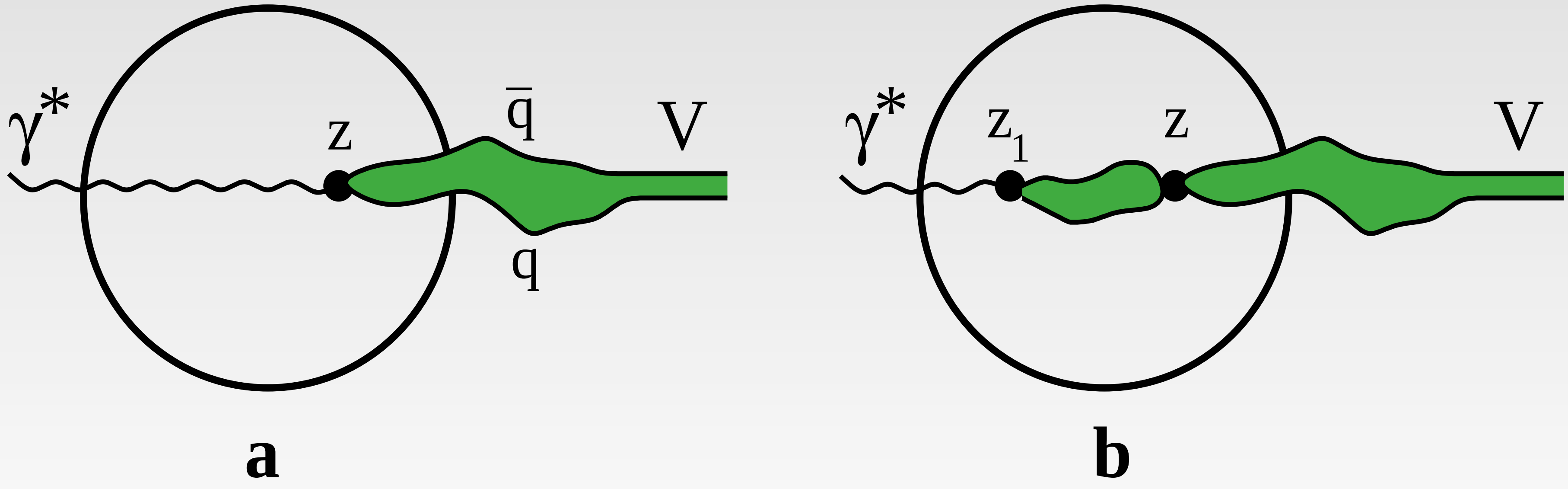

Basic formulas from the CDP

Different regimes of VM production (coh)

- If electroproduction of a vector meson leaves the target intact the process is usually called coherent or elastic. The mesons produced at different longitudinal coordinates and impact parameters add up coherently $\Rightarrow$ this simplifies the expressions for the integrated cross section,

$$\sigma_A^{coh} \equiv \sigma_{\gamma^* A \to VA}^{coh} = \int d^2 q \left| \int d^2 b \, e^{i\vec{q}\cdot\vec{b}} \, \mathcal{M}_{\gamma^* A \to VA}^{coh}(b) \right|^2 =$$

$$\int d^2 b \, | \mathcal{M}_{\gamma^* A \to VA}^{coh}(b) \, |^2 \, ,$$

Basic formulas from the CDP

Different regimes of VM production (coh)

- If electroproduction of a vector meson leaves the target intact the process is usually called coherent or elastic. The mesons produced at different longitudinal coordinates and impact parameters add up coherently ⇒ this simplifies the expressions for the integrated cross section,

$$\sigma_A^{coh} \equiv \sigma_{\gamma^* A \to V A}^{coh} = \int d^2 q \left| \int d^2 b \, e^{i\vec{q}\cdot\vec{b}} \, \mathcal{M}_{\gamma^* A \to V A}^{coh}(b) \right|^2 = \int d^2 b \, |\mathcal{M}_{\gamma^* A \to V A}^{coh}(b)\,|^2 \, ,$$

-

$$\mathcal{M}_{\gamma^* A \to V A}^{coh}(b) = \int_{-\infty}^{\infty} dz \, \rho_A(b,z) \, F_1(b,z) \, .$$

Basic formulas from the CDP

Different regimes of VM production **(coh)**

- In the high energy limit $l_c \gg R_A \Rightarrow$ $G(z_2, \vec{r}_2; z_1, \vec{r}_1) \to \delta(\vec{r}_2 - \vec{r}_1) \Rightarrow$ all fluctuations of the transverse $\bar{q}q$ separation are "frozen" by Lorentz time dilation and the nuclear amplitude squared has the form

$$\left|\mathcal{M}_{\gamma^* A \to V A}(b, s, Q^2)\right|^2_{l_c \gg R_A} =$$

$$4 \left| \int d^2 r \int_0^1 d\alpha \Psi_V^*(\vec{r}, \alpha) \left\{ 1 - \exp\left[-\frac{1}{2} \sigma_{\bar{q}q}(r, s) T_A(b) \right] \right\} \Psi_{\gamma^*}(\vec{r}, \alpha, Q^2) \right|^2$$

Gluon shadowing

- In the LC Green function approach the physical photon $|\gamma^*\rangle$ is decomposed into different Fock states, namely, the bare photon $|\gamma^*\rangle_0$, plus $|\bar{q}q\rangle$, $|\bar{q}qG\rangle$, etc.

Gluon shadowing

- In the LC Green function approach the physical photon $|\gamma^*\rangle$ is decomposed into different Fock states, namely, the bare photon $|\gamma^*\rangle_0$, plus $|\bar{q}q\rangle$, $|\bar{q}qG\rangle$, etc.
- The higher Fock states containing gluons describe the energy dependence of the VM production cross section on a nucleon, and also lead to GS in the nuclear case. However, these fluctuations are heavier and have a shorter coherence time (lifetime) than the lowest $|\bar{q}q\rangle$ state $\Rightarrow$ GS, which is related to the higher Fock states, will dominate at higher energies, i.e. at small values of $x \lesssim 0.01$.

Gluon shadowing

- In the LC Green function approach the physical photon $|\gamma^*\rangle$ is decomposed into different Fock states, namely, the bare photon $|\gamma^*\rangle_0$, plus $|\bar{q}q\rangle$, $|\bar{q}qG\rangle$, etc.
- The higher Fock states containing gluons describe the energy dependence of the VM production cross section on a nucleon, and also lead to GS in the nuclear case. However, these fluctuations are heavier and have a shorter coherence time (lifetime) than the lowest $|\bar{q}q\rangle$ state $\Rightarrow$ GS, which is related to the higher Fock states, will dominate at higher energies, i.e. at small values of $x \lesssim 0.01$.
- The nuclear shadowing for the $|\bar{q}q\rangle$ Fock component of the photon is dominated by the T photon polarizations, because the corresponding cross section is scanned at larger dipole sizes than for the L photon polarization.

Gluon shadowing

- The mean transverse $\bar{q}q$ separation is

$$\langle r \rangle \sim \frac{1}{\sqrt{Q^2\alpha(1-\alpha)+m_q^2}}$$

asymmetric pairs are suppressed by the distribution function of L photons $\Rightarrow$ smaller transverse size than fluctuations of T photons, $\langle r \rangle_L < \langle r \rangle_T$.

Gluon shadowing

- The mean transverse $\bar{q}q$ separation is

$$\langle r \rangle \sim \frac{1}{\sqrt{Q^2\alpha(1-\alpha)+m_q^2}}$$

asymmetric pairs are suppressed by the distribution function of L photons $\Rightarrow$ smaller transverse size than fluctuations of T photons, $\langle r \rangle_L < \langle r \rangle_T$.

- The leading-twist contribution for the shadowing of L photons arises from the $|\bar{q}qG\rangle$ Fock component of the photon because the gluon can propagate relatively far from the $\bar{q}q$ pair, although the $\bar{q}$-q separation is of the order $1/Q^2$. After radiation of the gluon the pair is in an octet state, and consequently the $|\bar{q}qG\rangle$ state represents a GG dipole. Then the corresponding correction to the longitudinal cross section is just gluon shadowing.

Gluon shadowing

- Although interpretations of GS depend on the reference frame and consequently are not Lorentz invariant, they represent the same phenomenon, related to the Lorentz invariant Reggeon graphs. The double- scattering correction to the cross section of gluon radiation can be expressed in Regge theory via the triple-Pomeron diagram. It is interpreted as a fusion of two Pomerons originated from different nucleons, $2\,I\!\!P \to I\!\!P$, which leads to a reduction of the nuclear gluon density G_A.

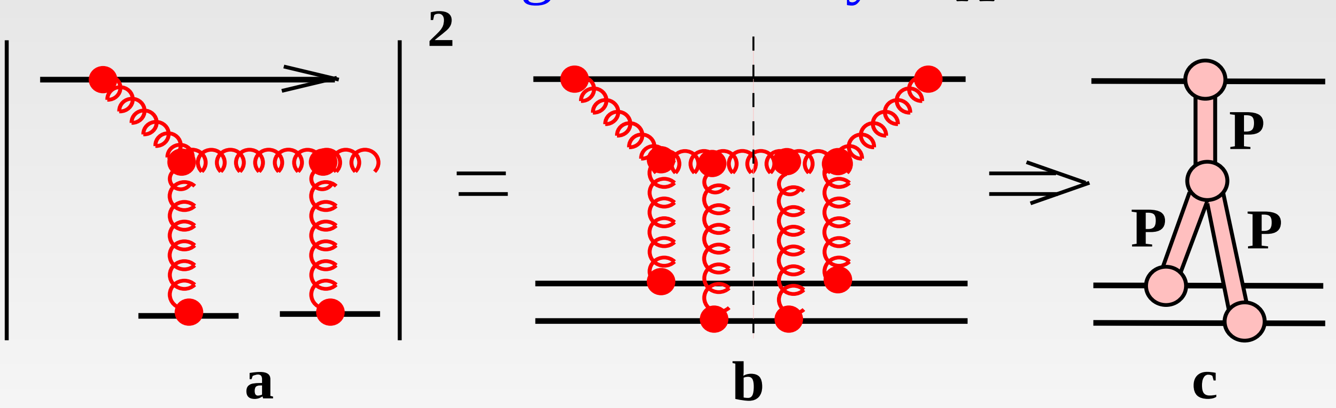

[The double scattering correction to gluon radiation in the rest frame of the target nucleus $(\mathbf{a})$. The absorptive part of the corresponding elastic pA amplitude $(\mathbf{b})$. The

Gluon shadowing

- GS can be identified as the shadowing correction to the L cross section coming from the GG dipole representing the $|\bar{q}qG\rangle$ Fock component of the photon.

Gluon shadowing

- GS can be identified as the shadowing correction to the L cross section coming from the GG dipole representing the $|\bar{q}qG\rangle$ Fock component of the photon.
- An important point for the evaluation of GS is knowing about the transverse size of this GG dipole. This size has been extracted from data for diffractive excitation of the incident hadrons to the states of large mass, the so called triple-Pomeron region. The mean dipole size of the GG system (radius of propagation of the LC gluons) is rather small , $r_0 \approx 0.3$ fm.

  [B.Z. Kopeliovich, A. Schäfer and A.V. Tarasov, *Phys. Rev.* **D62**, 054022 (2000)]

Gluon shadowing

- GS can be identified as the shadowing correction to the L cross section coming from the GG dipole representing the $|\bar{q}qG\rangle$ Fock component of the photon.
- An important point for the evaluation of GS is knowing about the transverse size of this GG dipole. This size has been extracted from data for diffractive excitation of the incident hadrons to the states of large mass, the so called triple-Pomeron region. The mean dipole size of the GG system (radius of propagation of the LC gluons) is rather small , $r_0 \approx 0.3$ fm.

  [B.Z. Kopeliovich, A. Schäfer and A.V. Tarasov, *Phys. Rev.* **D62**, 054022 (2000)]
- For calculation of GS we use the same LC Green function formalism.

Gluon shadowing

- We calculated the ratio of the gluon densities in nuclei and nucleon,

$$R_G(x,Q^2) = \frac{G_A(x,Q^2)}{A\,G_N(x,Q^2)} \approx 1 - \frac{\Delta\sigma_{tot}(\bar{q}qG)}{\sigma_{tot}^{\gamma^* A}}\,,$$

where $\Delta\sigma_{tot}(\bar{q}qG)$ is the inelastic correction to the total cross section $\sigma_{tot}^{\gamma^* A}$, related to the creation of a $|\bar{q}qG\rangle$ intermediate Fock state,

$$\Delta\sigma_{tot}(\bar{q}qG) = \mathrm{Re}\int\limits_{-\infty}^{\infty} dz_2 \int\limits_{-\infty}^{z_2} dz_1\, \rho_A(b,z_1)\,\rho_A(b,z_2) \times$$

$$\int d^2x_2\, d^2y_2\, d^2x_1\, d^2y_1 \int d\alpha_q \frac{d\,\alpha_G}{\alpha_G} F^{\dagger}_{\gamma^*\to\bar{q}qG}(\vec{x}_2,\vec{y}_2,\alpha_q,\alpha_G) \times$$

$$G_{\bar{q}qG}(\vec{x}_2,\vec{y}_2,z_2;\vec{x}_1,\vec{y}_1,z_1)\, F_{\gamma^*\to\bar{q}qG}(\vec{x}_1,\vec{y}_1,\alpha_q,\alpha_G)\,.$$

Gluon shadowing

- $F_{\gamma^*\to\bar{q}qG}$ is the amplitude of diffractive $\bar{q}qG$ production in a $\gamma^* N$ interaction, and it is given by

$$F_{\gamma^*\to\bar{q}qG}(\vec{x},\vec{y},\alpha_q,\alpha_G) = \frac{9}{8}\,\Psi_{\bar{q}q}(\alpha_q,\vec{x}-\vec{y}) \times$$

$$\left[\Psi_{qG}\left(\frac{\alpha_G}{\alpha_q},\vec{x}\right) - \Psi_{\bar{q}G}\left(\frac{\alpha_G}{1-\alpha_q},\vec{y}\right)\right]\left[\sigma_{\bar{q}q}(x)+\sigma_{\bar{q}q}(y)-\sigma_{\bar{q}q}(\vec{x}-\vec{y})\right],$$

where $\Psi_{\bar{q}q}$ and $\Psi_{\bar{q}G}$ are the LC distrib. functions of the $\bar{q}q$ fluctuations of a photon and qG fluctuations of a quark.

Gluon shadowing

- $F_{\gamma^*\to\bar{q}qG}$ is the amplitude of diffractive $\bar{q}qG$ production in a $\gamma^* N$ interaction, and it is given by

$$F_{\gamma^*\to\bar{q}qG}(\vec{x},\vec{y},\alpha_q,\alpha_G) = \frac{9}{8}\,\Psi_{\bar{q}q}(\alpha_q,\vec{x}-\vec{y}) \times$$

$$\left[\Psi_{qG}\left(\frac{\alpha_G}{\alpha_q},\vec{x}\right) - \Psi_{\bar{q}G}\left(\frac{\alpha_G}{1-\alpha_q},\vec{y}\right)\right]\left[\sigma_{\bar{q}q}(x)+\sigma_{\bar{q}q}(y)-\sigma_{\bar{q}q}(\vec{x}-\vec{y})\right],$$

  where $\Psi_{\bar{q}q}$ and $\Psi_{\bar{q}G}$ are the LC distrib. functions of the $\bar{q}q$ fluctuations of a photon and qG fluctuations of a quark.
- $G_{\bar{q}qG}(\vec{x}_2,\vec{y}_2,z_2;\vec{x}_1,\vec{y}_1,z_1)$ is the LC Green function describing the propagation of the $\bar{q}qG$ system from the initial state with longitudinal and transverse coordinates z_1 and $\vec{x}_1,\vec{y}_1$, to the final coordinates $(z_2,\vec{x}_2,\vec{y}_2)$. For the calculation of GS one should suppress the intrinsic $\bar{q}q$ separation, i.e. assume $\vec{x}=\vec{y}$ - GF simplifies and describes the propagation of a G-G dipole through a medium.

Gluon shadowing

- There is a strong nonperturbative interaction which squeezes the G-G wave packet and substantially diminishes gluon shadowing. The smallness of the G-G transverse separation is not a model assumption, but is dictated by data for hadronic diffraction into large masses (triple-Pomeron regime).

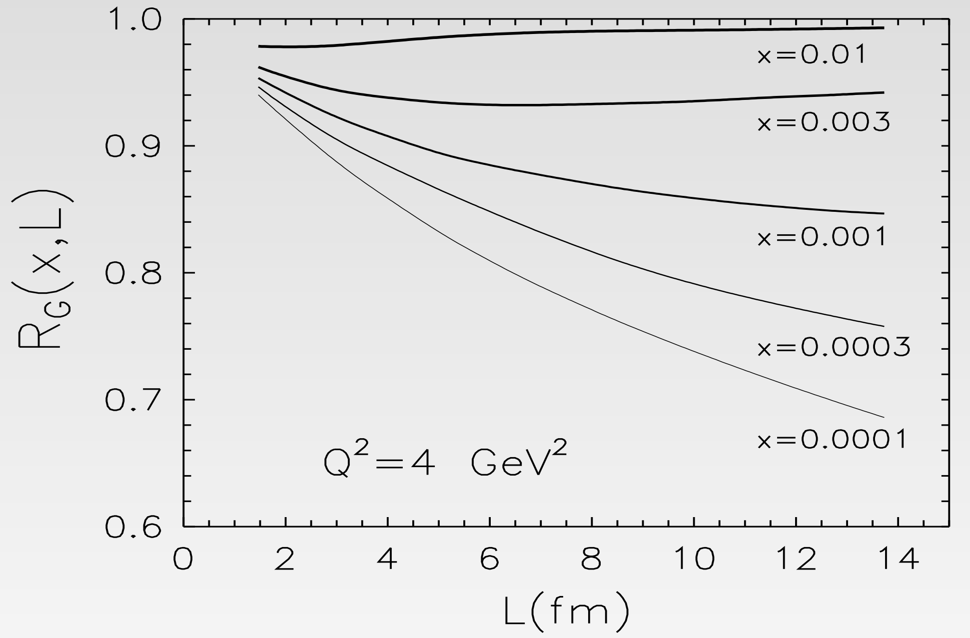

[The ratio of the nucleus-to-nucleon gluon densities as function of the thickness of the nucleus, $L = T(b)/\rho_0$, at $Q^2 = 4$ GeV^2 and different fixed values of x.]

Gluon shadowing

Gluon shadowing as function of different variables

Gluon shadowing

Gluon shadowing as function of different variables

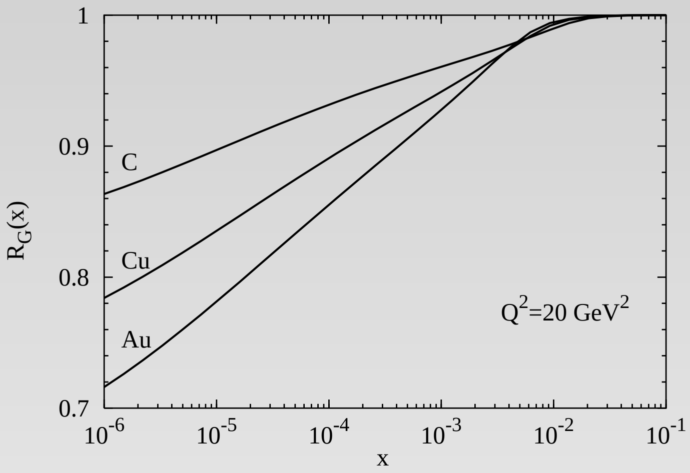

Gluon shadowing

Gluon shadowing as function of different variables

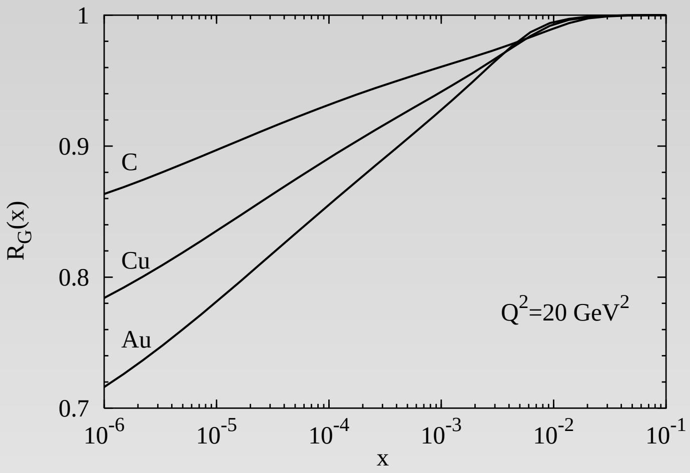

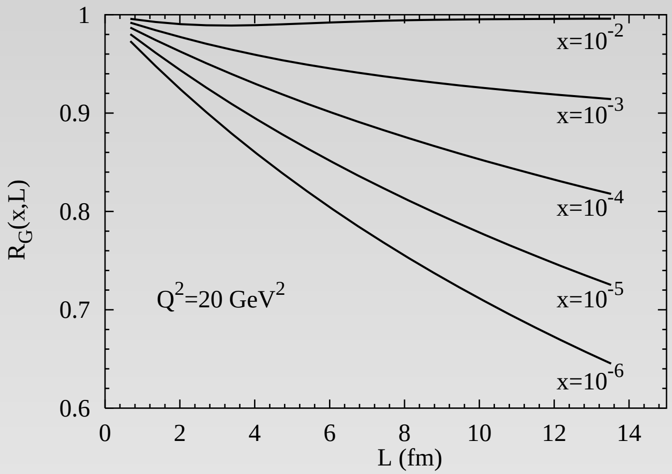

Gluon shadowing

Gluon shadowing as function of different variables

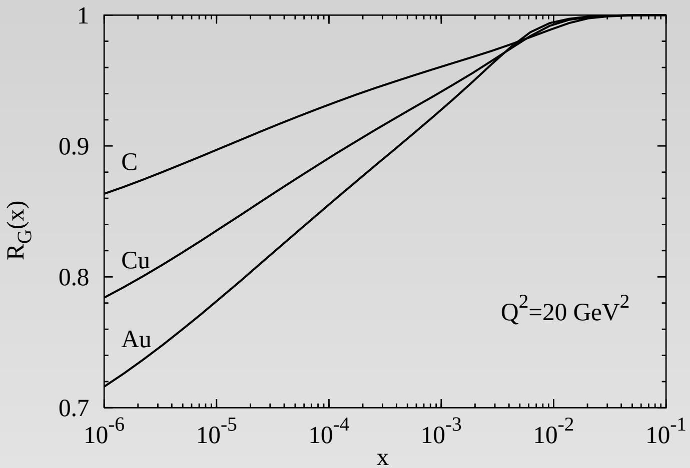

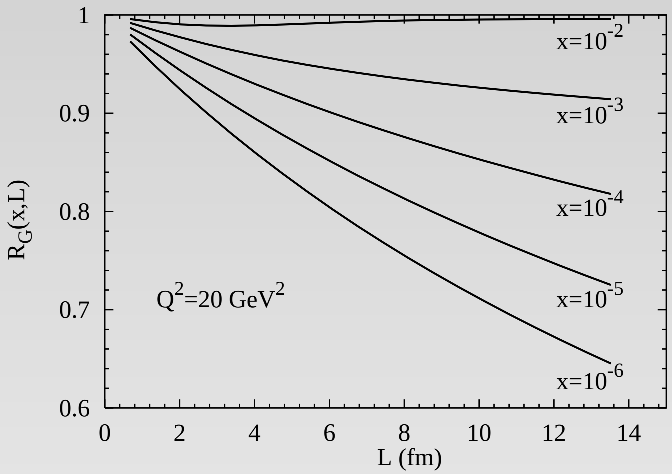

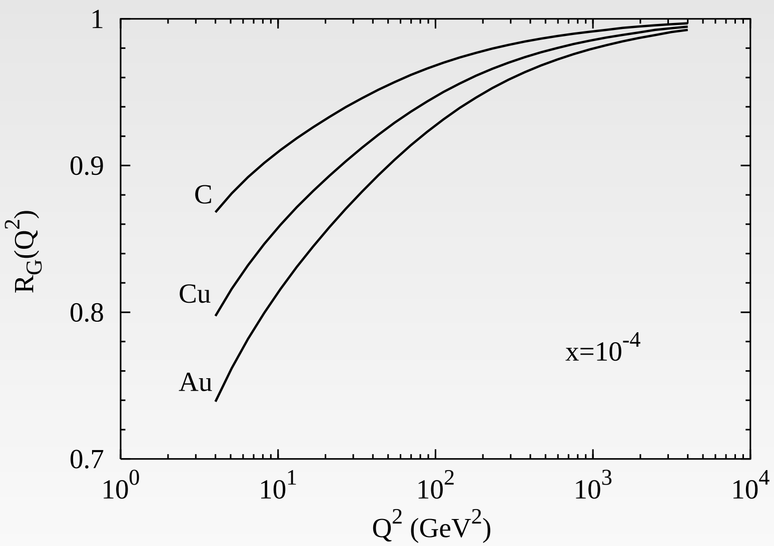

Numerical results vs. data

Comparison with CLAS data

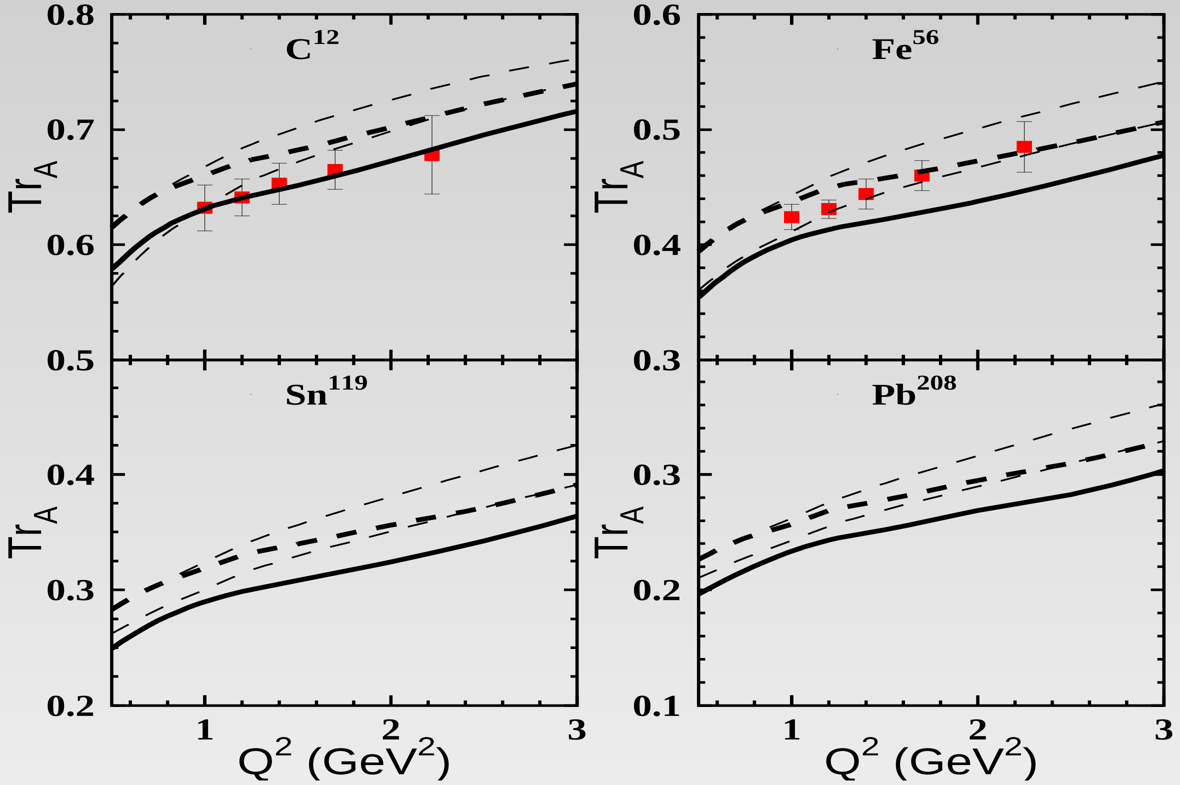

$Tr_A^{inc}(Q^2)$ for exclusive electroproduction of ρ on ^{12}C, ^{56}Fe, ^{119}Sn and ^{207}Pb targets.

The thin dashed lines $\Leftrightarrow$ fixed $l_c = 0.5$ and 0.8 fm from bottom to top. The solid lines represent predictions including corrections for the ρ meson decay in the nucleus. The thick lines reflects the real $Q^2 - l_c$ correlation $\Leftrightarrow$ CLAS experiment

[CLAS Collaboration, L. El Fassi et al., *Phys. Lett.* **B712**, 326 (2012)]

Numerical results vs. data

Comparison with CLAS data

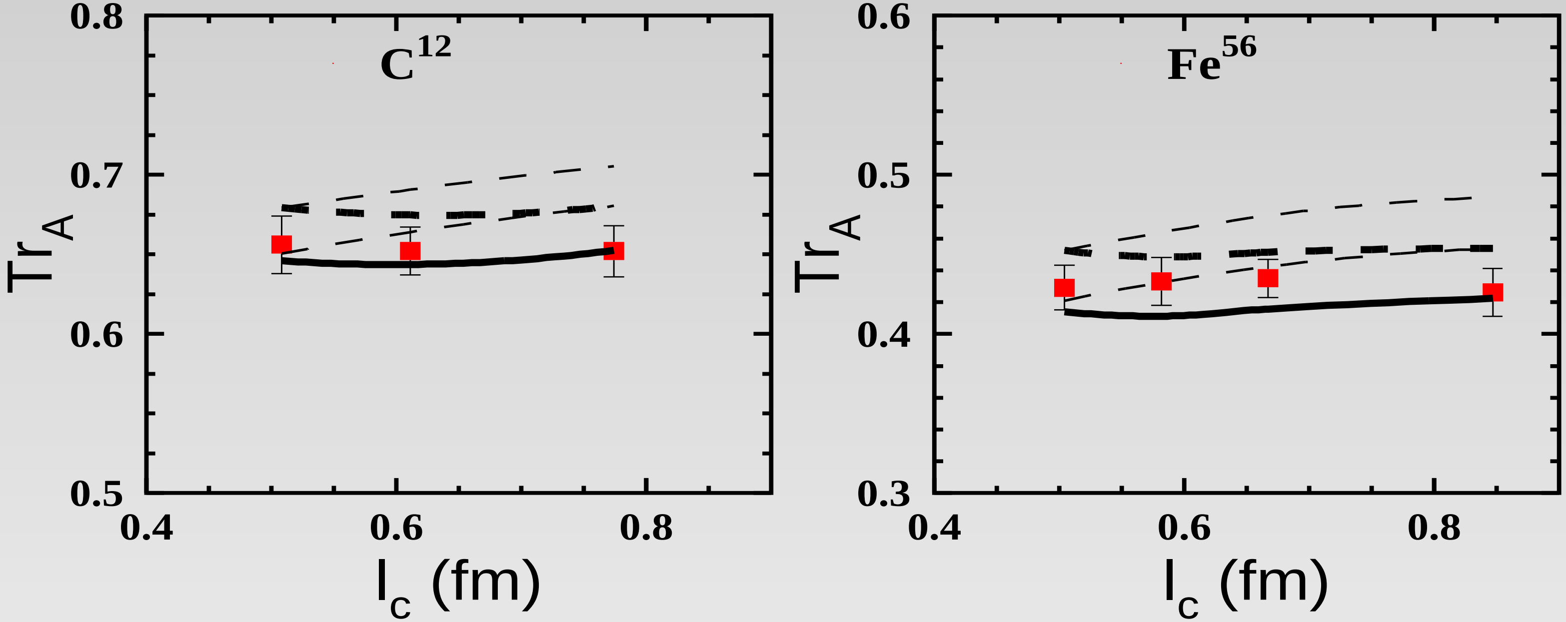

$Tr_A^{inc}(l_c)$ for exclusive electroproduction of ρ mesons on ^{12}C and ^{56}Fe. The thin dashed lines represent the Q^2 values fixed at $Q^2 = 1.2\ \mathrm{GeV}^2$ (^{12}C target) resp. $Q^2 = 1.1\ \mathrm{GeV}^2$ (^{56}Fe target) and $Q^2 = 1.6\ \mathrm{GeV}^2$ from bottom to top. The solid lines represent predictions including corrections for the ρ meson decay in the nucleus. The thick lines reflects the real $l_c - Q^2$ correlation corresponding to CLAS experiment.

[CLAS Collaboration, L. El Fassi et al., *Phys. Lett.* **B712**, 326 (2012)]

Numerical results vs. data

Comparison with CLAS data

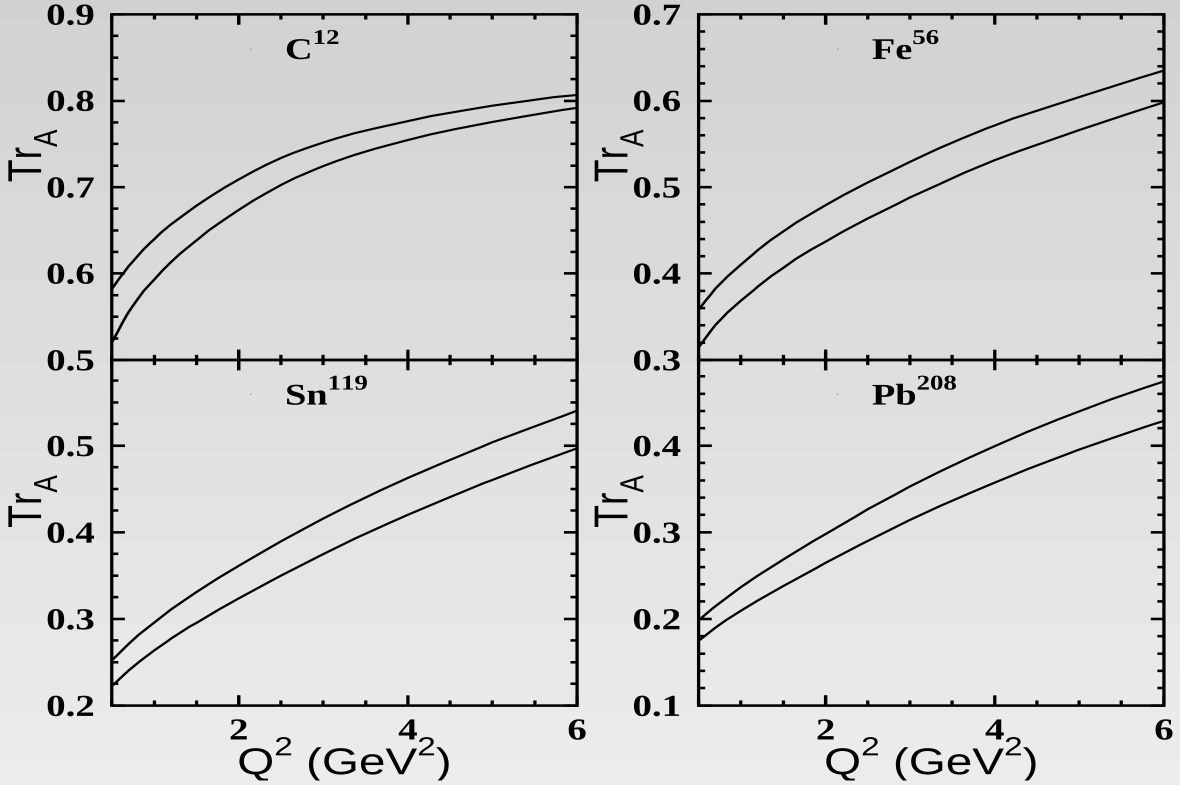

$Tr_A^{inc}(Q^2)$ for exclusive electroproduction of ρ on ^{12}C, ^{56}Fe, ^{119}Sn and ^{207}Pb targets corresponding to JLab upgrade to **12 GeV electron beam**. The lines represent predictions including corrections for the ρ meson decay in the nucleus and $\Leftrightarrow$ $l_c = 0.5$ and 0.8 fm from bottom to top.

Numerical results vs. data

Comparison with HERMES data

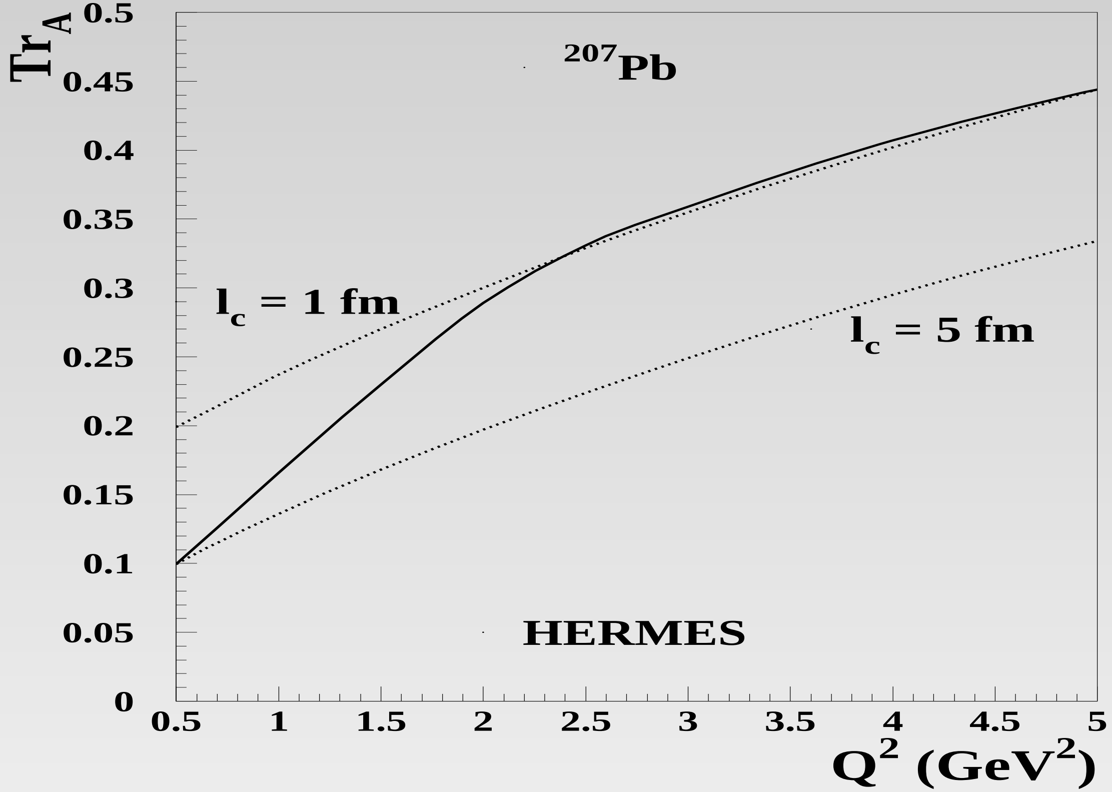

Tr_A^{inc} for exclusive electroproduction of ρ mesons on ^{207}Pb target. The dotted lines represent the CL fixed at $l_c = 1.0$ and 5.0 fm. The solid lines represent predictions at the fixed mean $\langle \nu \rangle = 13$ GeV corresponding to HERMES experiment.

[B.Z. Kopeliovich, J. Nemchik, I. Schmidt, *Phys. Rev.* **C76**, 015205 (2007)]

Numerical results vs. data

Comparison with HERMES data

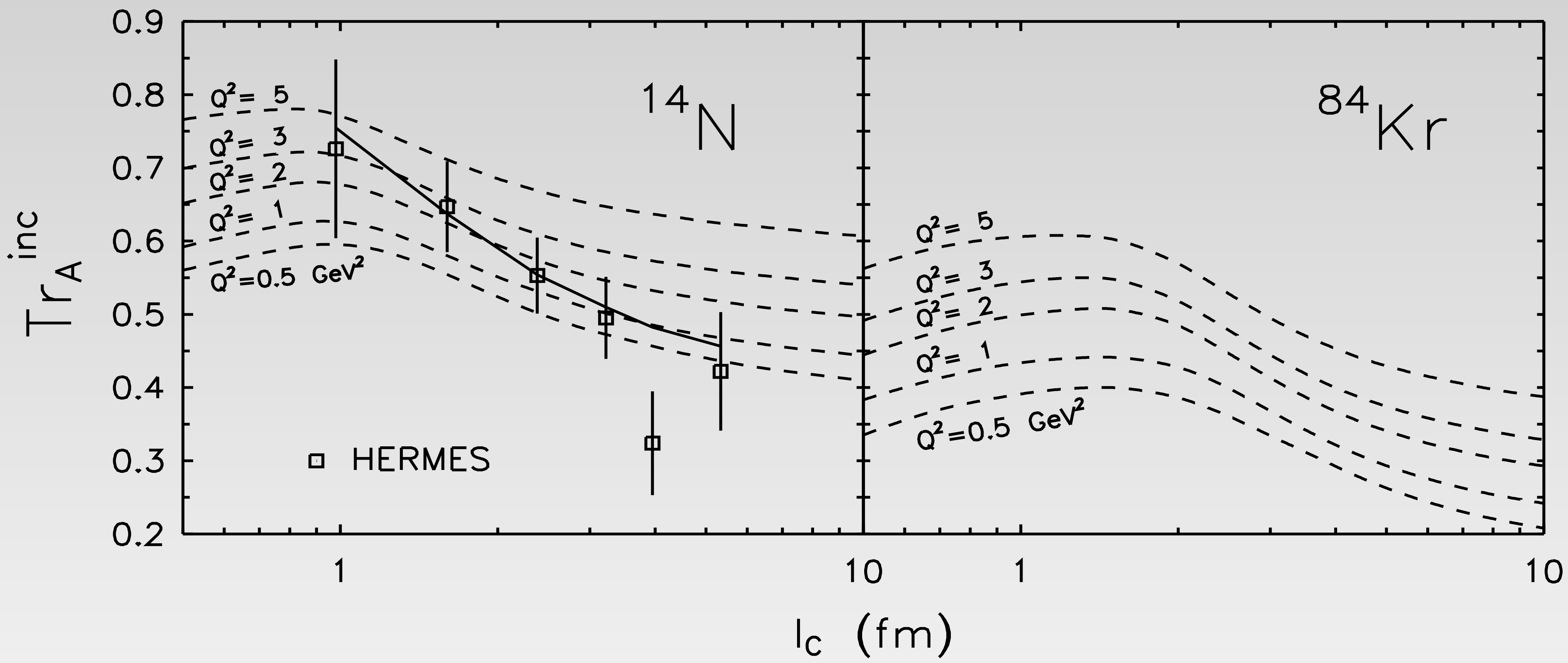

$\boldsymbol{Tr_A}$ for incoherent electroproduction of $\boldsymbol{\rho}$ off $^{14}\boldsymbol{N}$ and $^{84}\boldsymbol{Kr}$ as function of $\boldsymbol{l_c}$ at fixed $\boldsymbol{Q^2}$ The solid curve is calculated at the mean values of $\boldsymbol{l_c}$ and $\boldsymbol{Q^2}$ corresponding to each exp. point

[B.Z. Kopeliovich, J. Nemchik, A. Schaefer, A.V. Tarasov, *Phys. Rev.* **C65**, 035201 (2002)]

Numerical results vs. data

Comparison with E665 data

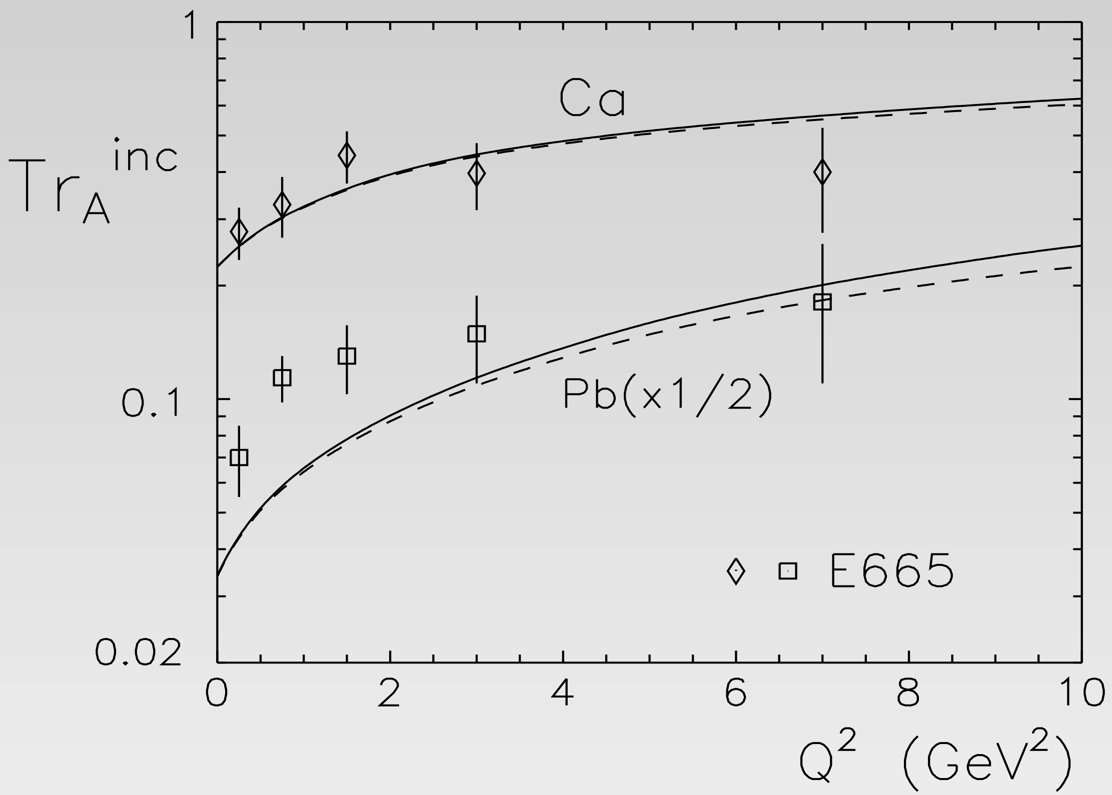

Solid and dashed curves show our results using the LC Green function approach and the "frozen" approximation

[B.Z. Kopeliovich, J. Nemchik, A. Schaefer, A.V. Tarasov, *Phys. Rev.* **C65**, 035201 (2002)]

Numerical results vs. data

Comparison with E665 data

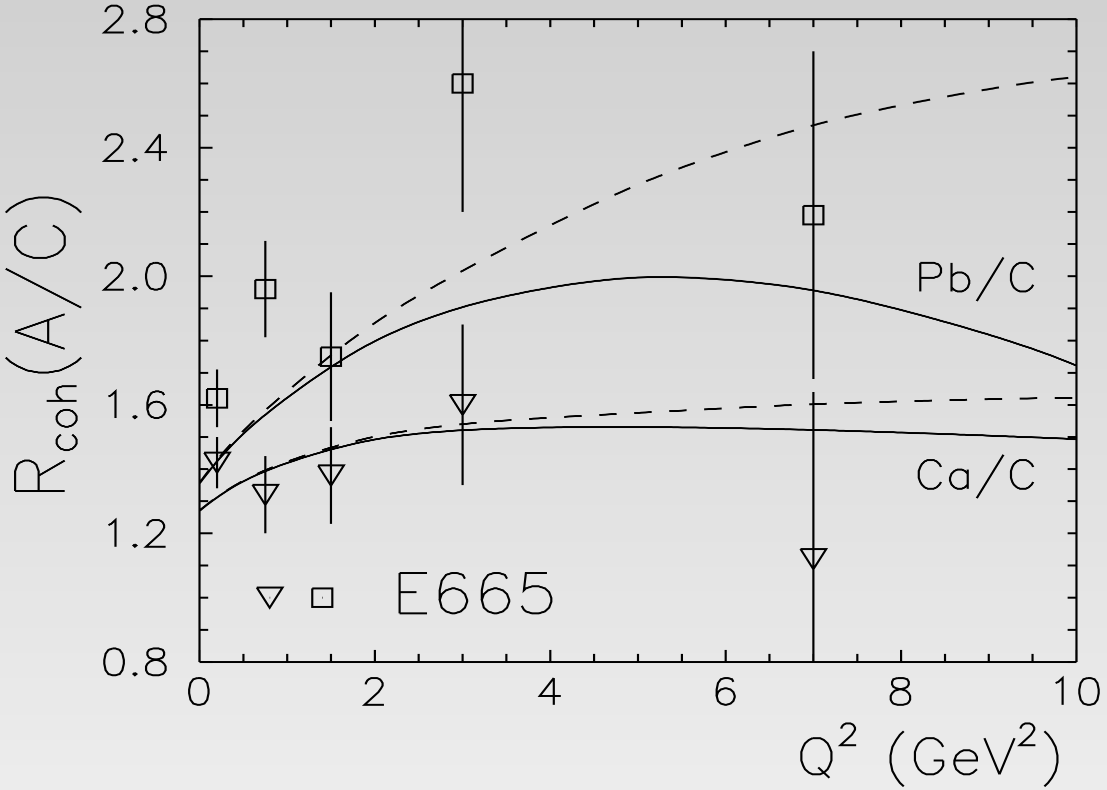

Solid and dashed curves show our results using the LC Green function approach and the “frozen” approximation

[B.Z. Kopeliovich, J. Nemchik, A. Schaefer, A.V. Tarasov, *Phys. Rev.* **C65**, 035201 (2002)]

Numerical results vs. data

Comparison with NMC data

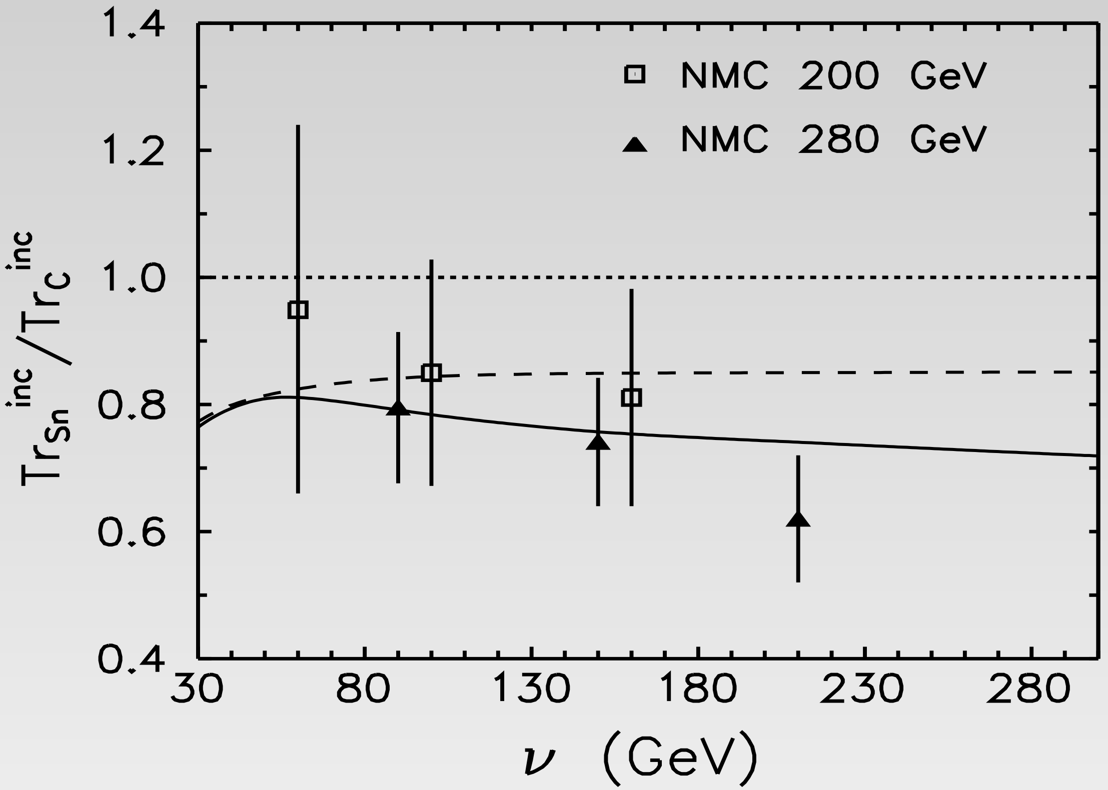

Solid and dashed curves show our results using the LC Green function approach with no restriction for l_c, l_f and in the limit of

$$l_c \longrightarrow 0$$

[J. Nemchik, *Phys. Rev.* **C66**, 045204 (2002)]

Numerical results

Perspectives for EIC

Incoherent production of light vector mesons

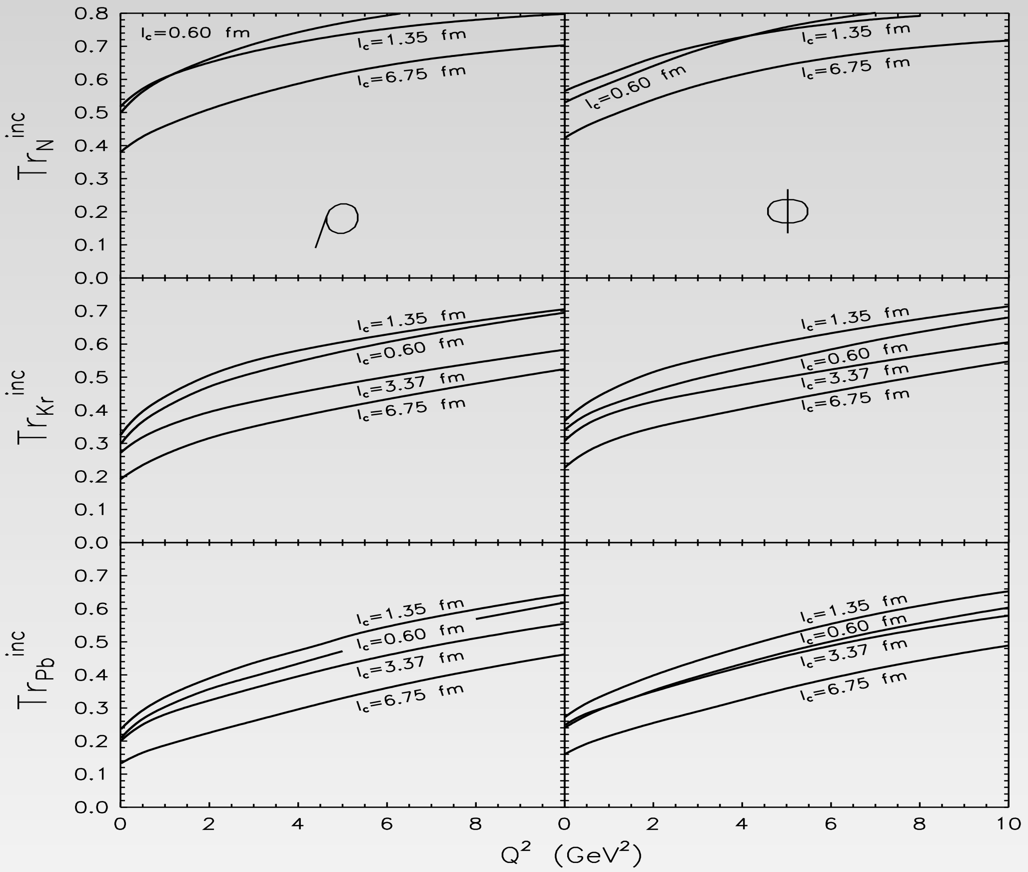

Cond. $\boldsymbol{l_c \gg R_A}$ should be fulfilled for $\boldsymbol{Q^2 \lesssim 100 \div 150}$ GeV$^{\mathbf{2}}$

$\Rightarrow$ investigation of a stronger onset of CT effects

[B.Z. Kopeliovich, J. Nemchik, A. Schaefer, A.V. Tarasov, *Phys. Rev.* **C65**, 035201 (2002)]

Numerical results

Perspectives for EIC

Coherent production of light vector mesons

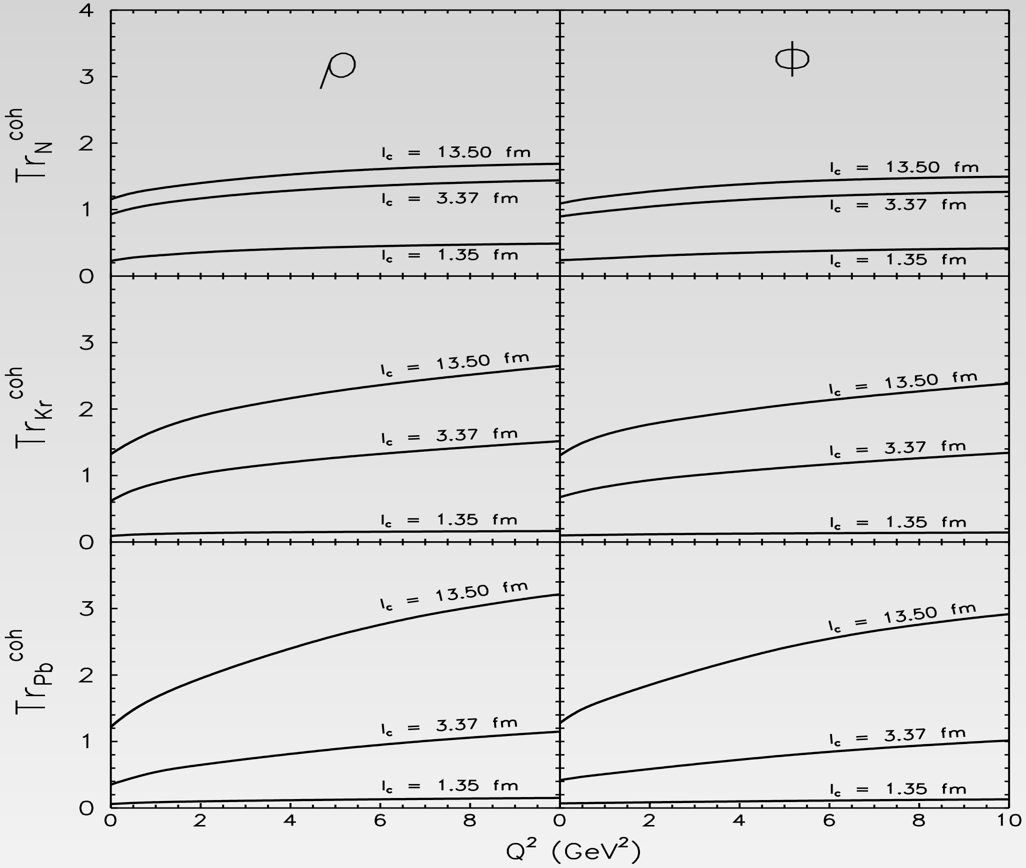

Cond. $\boldsymbol{l_c \gg R_A}$ should be fulfilled for $\boldsymbol{Q^2 \lesssim 100 \div 150}$ GeV$^{\mathbf{2}}$

$\Rightarrow$ investigation of a stronger onset of CT effects

[B.Z. Kopeliovich, J. Nemchik, A. Schaefer, A.V. Tarasov, *Phys. Rev.* **C65**, 035201 (2002)]

Numerical results

Perspectives for EIC

Production of light vector mesons - energy dependence

[B.Z. Kopeliovich, J. Nemchik, A. Schaefer, A.V. Tarasov, *Phys. Rev.* **C65**, 035201 (2002)]

Numerical results

Perspectives for EIC

Production of light vector mesons - energy dependence

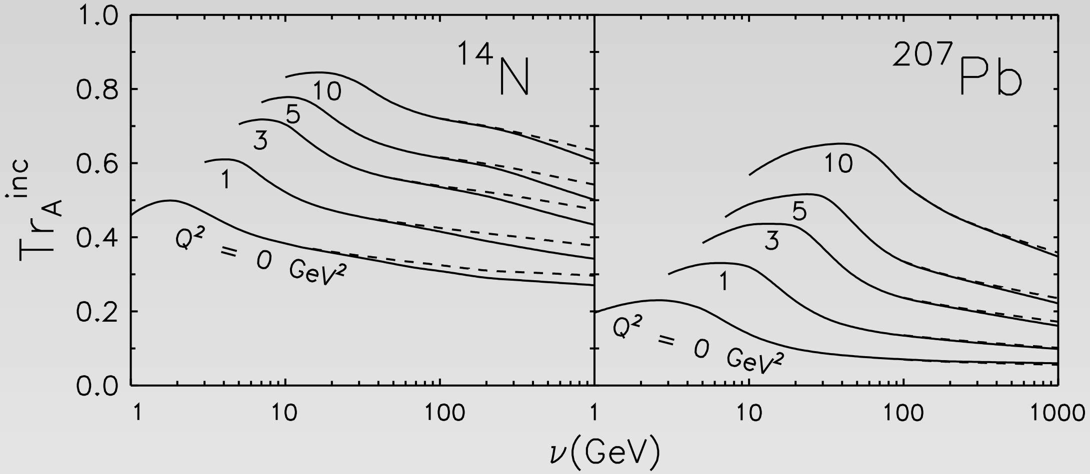

[B.Z. Kopeliovich, J. Nemchik, A. Schaefer, A.V. Tarasov, *Phys. Rev.* **C65**, 035201 (2002)]

Numerical results

Perspectives for EIC

Production of light vector mesons - energy dependence

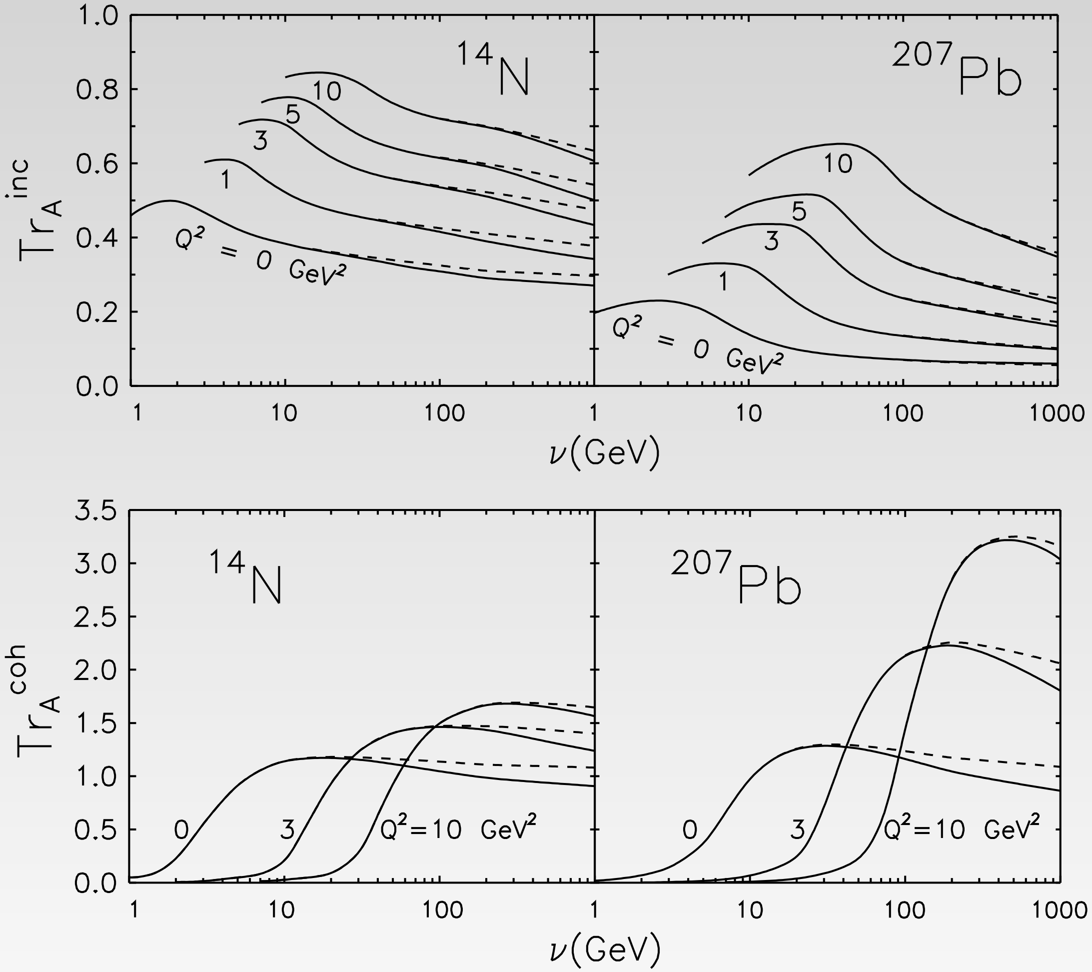

[B.Z. Kopeliovich, J. Nemchik, A. Schaefer, A.V. Tarasov, *Phys. Rev.* **C65**, 035201 (2002)]

Numerical results

Perspectives for EIC

Incoherent and coherent production of J/Ψ

[J. Nemchik, *Phys. Rev.* **C66**, 045204 (2002)]

Numerical results

Perspectives for EIC

Incoherent and coherent production of J/Ψ

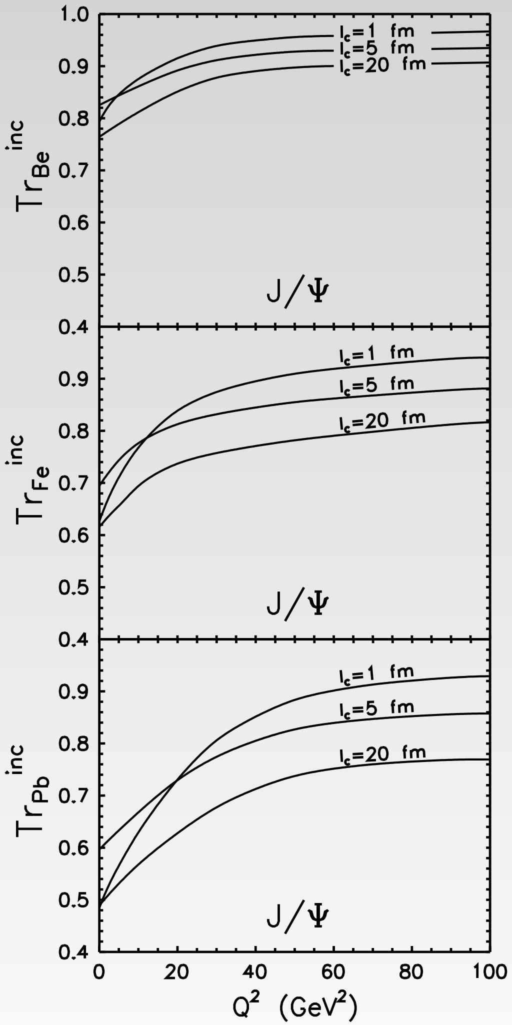

[J. Nemchik, *Phys. Rev.* **C66**, 045204 (2002)]

Numerical results

Perspectives for EIC

Incoherent and coherent production of J/Ψ

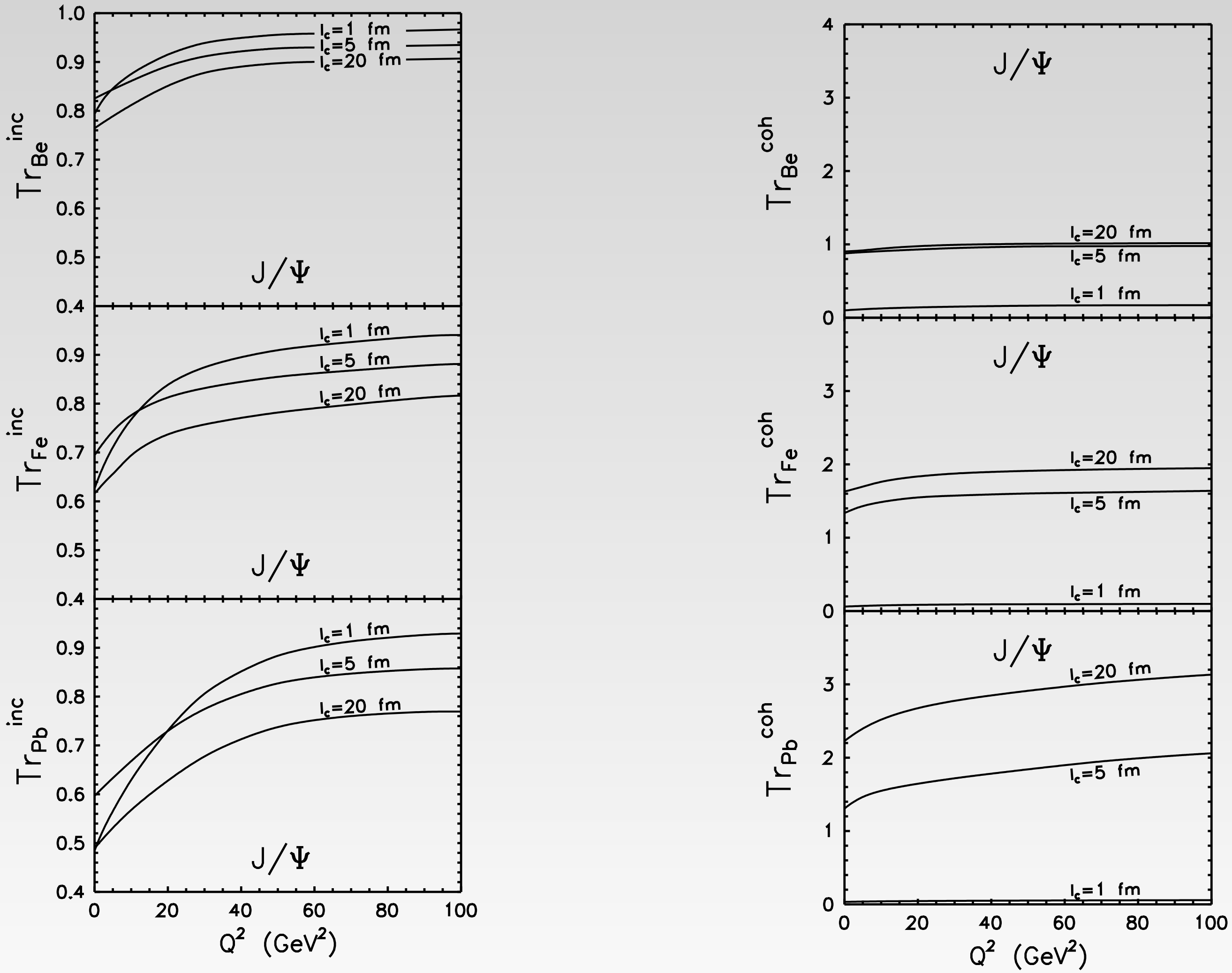

[J. Nemchik, *Phys. Rev.* **C66**, 045204 (2002)]

Numerical results

Perspectives for EIC

Production of J/Ψ - energy dependence

[J. Nemchik, *Phys. Rev.* **C66**, 045204 (2002)]

Numerical results

Perspectives for EIC

Production of J/Ψ - energy dependence

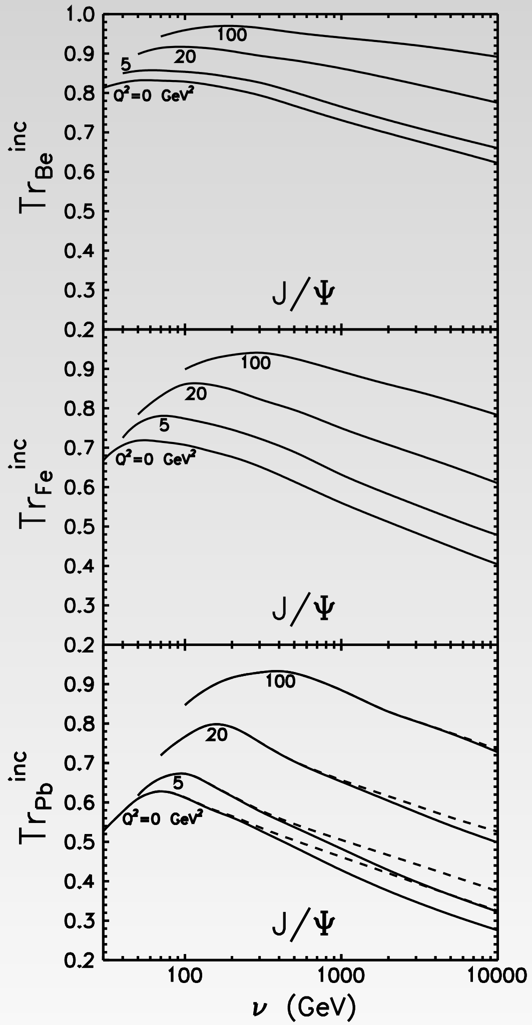

[J. Nemchik, *Phys. Rev.* **C66**, 045204 (2002)]

Numerical results

Perspectives for EIC

Production of J/Ψ - energy dependence

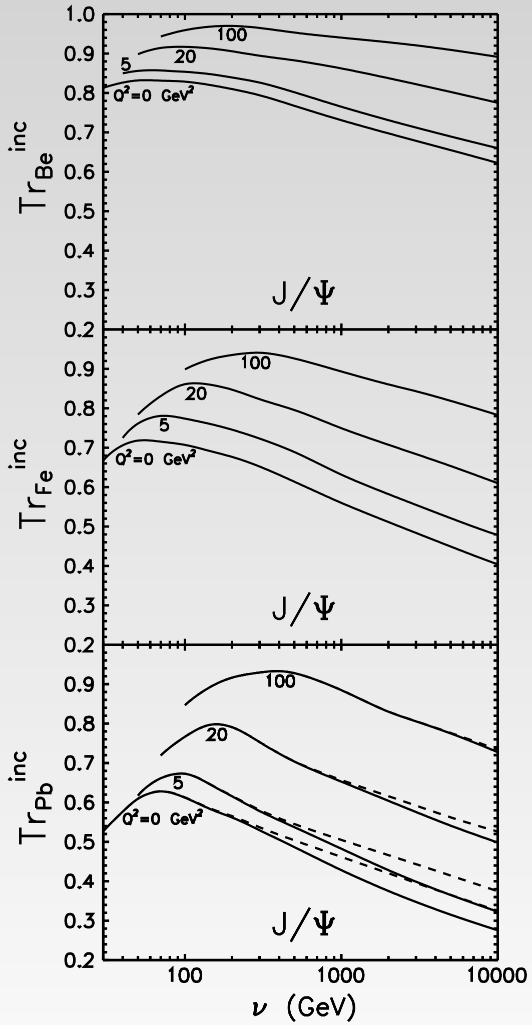

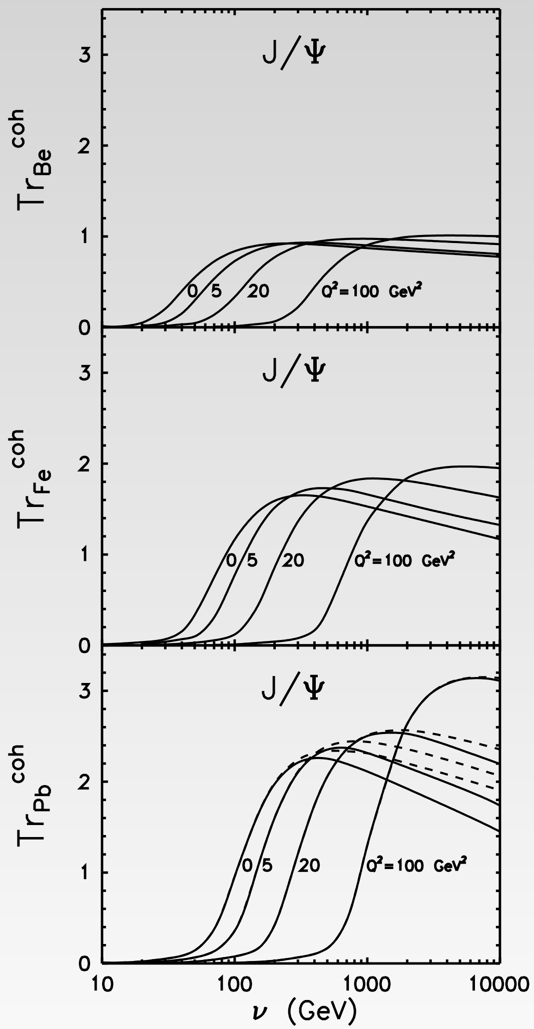

[J. Nemchik, *Phys. Rev.* **C66**, 045204 (2002)]

Summary

- Electroproduction of vector mesons off nuclei is a very effective tool for studying the interplay between coherence (shadowing) and formation (color transparency) effects.

Summary

- Electroproduction of vector mesons off nuclei is a very effective tool for studying the interplay between coherence (shadowing) and formation (color transparency) effects.
- We investigated the manifestation of these effects at different energies with the main respect to EIC kinematic region using a rigorous quantum-mechanical approach based on the light-cone QCD Green function formalism.

Summary

- Electroproduction of vector mesons off nuclei is a very effective tool for studying the interplay between coherence (shadowing) and formation (color transparency) effects.
- We investigated the manifestation of these effects at different energies with the main respect to EIC kinematic region using a rigorous quantum-mechanical approach based on the light-cone QCD Green function formalism.
- We studied the onset of CT effects at different energies, predicting a rising nuclear transparency as a function of Q^2 in a good agreement with data from the CLAS HERMES, E665 and NMC Collaborations.

Summary

- At low and medium energies the onset of CT effect is usually infected by CL effects (shadowing) and both effects work in the same (opposite) direction for incoherent (coherent) electroproduction of vector mesons.

Summary

- At low and medium energies the onset of CT effect is usually infected by CL effects (shadowing) and both effects work in the same (opposite) direction for incoherent (coherent) electroproduction of vector mesons.
- For elimination of CL effects when $l_c \lesssim R_A$, is unavoidable to study a rising nuclear transparency as function of Q^2 for fixed l_c

[B.Z. Kopeliovich, J. Nemchik, A. Schaefer and A.V. Tarasov, *P.R.* **C65**, 035201 (2002).]

Summary

- At low and medium energies the onset of CT effect is usually infected by CL effects (shadowing) and both effects work in the same (opposite) direction for incoherent (coherent) electroproduction of vector mesons.
- For elimination of CL effects when $l_c \lesssim R_A$, is unavoidable to study a rising nuclear transparency as function of Q^2 for fixed l_c

[B.Z. Kopeliovich, J. Nemchik, A. Schaefer and A.V. Tarasov, *P.R.* **C65**, 035201 (2002).]

- In the CLAS energy range, both $l_c, l_f \ll R_A \Rightarrow$ the CL effects are much weaker than the observed effect of CT. Thus one can investigate the onset of CT studying the rise of Tr_A with Q^2 at fixed photon energies, processing the data at maximal statistics. Such a procedure allows to reach much higher Q^2 effective for studying the CT phenomenon, than those used in the HERMES experiment applying the CL-elimination prescription of fixing l_c.

Summary

- At large energies corresponding to EIC, the high energy limit, $l_f \sim l_c \gg R_A$ can be reached for a broad range of photon virtualities, $Q^2 \lesssim 100 \div 150$ GeV^2 for ρ^0, Φ^0, J/Ψ and $Q^2 \lesssim 50 \div 100$ GeV^2 for Υ $\Rightarrow$ this so called “frozen” approximation includes only CT, because there are no fluctuations of the transverse size of the $\bar{q}q$ pair.

Summary

- At large energies corresponding to EIC, the high energy limit, $l_f \sim l_c \gg R_A$ can be reached for a broad range of photon virtualities, $Q^2 \lesssim 100 \div 150\ \mathrm{GeV}^2$ for ρ^0, Φ^0, J/Ψ and $Q^2 \lesssim 50 \div 100\ \mathrm{GeV}^2$ for $\Upsilon \Rightarrow$ this so called “frozen” approximation includes only CT, because there are no fluctuations of the transverse size of the $\bar{q}q$ pair.
- The effects of gluon shadowing were shown to be important at high energies corresponding to EIC. Nuclear suppression of gluons was calculated within the same LC Green function formalism and included in predictions.

Summary

- At large energies corresponding to EIC, the high energy limit, $l_f \sim l_c \gg R_A$ can be reached for a broad range of photon virtualities, $Q^2 \lesssim 100 \div 150$ GeV^2 for ρ^0, Φ^0, J/Ψ and $Q^2 \lesssim 50 \div 100$ GeV^2 for Υ $\Rightarrow$ this so called "frozen" approximation includes only CT, because there are no fluctuations of the transverse size of the $\bar{q}q$ pair.
- The effects of gluon shadowing were shown to be important at high energies corresponding to EIC. Nuclear suppression of gluons was calculated within the same LC Green function formalism and included in predictions.
- Investigation of energy dependence of nuclear transparency especially in production of heavy vector mesons allows to study interplay between CT and CL effects at different values of Q^2.

Summary

- At large energies corresponding to EIC, the high energy limit, $l_f \sim l_c \gg R_A$ can be reached for a broad range of photon virtualities, $Q^2 \lesssim 100 \div 150\ \mathrm{GeV}^2$ for ρ^0, Φ^0, J/Ψ and $Q^2 \lesssim 50 \div 100\ \mathrm{GeV}^2$ for Υ $\Rightarrow$ this so called "frozen" approximation includes only CT, because there are no fluctuations of the transverse size of the $\bar{q}q$ pair.
- The effects of gluon shadowing were shown to be important at high energies corresponding to EIC. Nuclear suppression of gluons was calculated within the same LC Green function formalism and included in predictions.
- Investigation of energy dependence of nuclear transparency especially in production of heavy vector mesons allows to study interplay between CT and CL effects at different values of Q^2.
- Investigation of Q^2 dependence of almost sarurated values of Tr_A^{coh} and Tr_A^{inc} at high energies corresponding to EIC represents an alternative way for study of CT effects.